Effect of forest conversion to oil palm plantations on carbon dioxide balance in tropical peatlands

（熱帯泥炭林のオイルパームプランテーションへの土地利用変化が二酸化炭素収支に与える影響）

Hokkaido University, Graduate School of Agriculture

Division of Environmental Resources Doctoral Course

Frankie Kiew

ABSTRACT

Over millennia, tropical peat swamp forest (PSF) has stored a large amount of carbon (C) both in biomass and soil. Currently, however, this C-rich ecosystem is exposed to disturbances related to land-use change. For example, the large distribution of PSF in southeast Asia chiefly in Indonesia and Malaysia has been affected by the rapid expansion of oil palm plantations (OPP). Other than significant changes in vegetation, plantations need drainage for lowering groundwater level (GWL) to keep better palm growth and potentially enhances oxidative peat decomposition. In order to understand the environmental impact of OPP from the view point of global warming, it is crucial to assess the change of carbon dioxide (CO_2) balance through the PSF conversion. To date, however, no study has reported the net ecosystem CO_2 exchange (NEE) of OPP established on peat. The objectives of this study are: (a) to monitor NEE of a PSF and an OPP in Sarawak, Malaysia by the eddy covariance technique, (b) to investigate the controlling factors of CO_2 fluxes, and (c) to quantify the annual CO_2 balances of the two sites and compare them to discuss the effect of the land-use change on ecosystem CO_2 balance.

1. Carbon dioxide fluxes above a peat swamp forest.

NEE has been measured above a relatively drained secondary PSF since 2010. NEE was partitioned into respiration (RE) and photosynthesis (GPP) using an empirical method. RE differ significantly in the dry and wet periods ($p < 0.01$). However, no significant difference was found in GPP. Thus, the seasonal difference in NEE (0.52 g C m^{-2} d^{-1}) was mainly attributable to that in RE (0.57 g C m^{-2} d^{-1}). Lower GWL in the dry period was the main cause for greater RE, because lower GWL enhances peat aeration and potentially increases oxidative peat decomposition. Mean (± 1 standard deviation) of annual NEE, RE and GPP were −136 ± 51, 3546 ± 149, and 3682 ± 149 g C m^{-2} yr^{-1} for four years until 2014. The annual NEE was comparable to those of some tropical rain forests on mineral soil.

Aboveground biomass (AGB) was estimated at 140 and 146 t ha^{-1}, respectively, in 2016 and 2017. Mean soil C content at 0-25 cm and 25-50 cm depths from 2011 to 2014 were estimated at 52.2 ± 0.7% and 53.9 ± 0.7% respectively.

2. Carbon dioxide fluxes on an oil palm plantation

NEE has also measured above an OPP established in 2004. GWL in OPP (-60 cm) was much lower than in PSF (-17.6 cm) on average and was relatively stable, because GWL was controlled by ditches. Similarly, soil moisture was maintained at around 0.56 m^3 m^{-3}. RE showed no significant relationship with GWL but was positively correlated with soil moisture ($P < 0.001$). Mean annual NEE, RE and GPP from 2011 to 2014 were estimated at 1034 ± 229, 3663 ± 182, 2630 ± 106 g C m^{-2} yr^{-1}, respectively. AGB was estimated at 21.4 and 54.2 t ha^{-1}, respectively, in March 2011 and July 2014. Soil C content measured annually from 2011 to 2014 were 55.3 ± 0.8% and 56.4 ± 1.0%, respectively, at 0-25 and 25-50 cm.

3. Effect of land conversion on ecosystem-scale carbon dioxide balance

The annual NEE was negative in PSF (a moderate CO_2 sink) but positive in OPP (a large CO_2 source). In contrast, annual RE values were similar each other, though it was expected to increase after the land conversion owing to lowered GWL and much woody debris left on the ground. The unchanged RE was probably caused by less autotrophic respiration due to much less AGB in OPP than in PSF. Thus, the large CO_2 emissions from OPP was attributable to 26% reduction in annual GPP mainly because of less AGB.

ACKNOWLEDGEMENTS

This thesis only successful with kind support and help from many parties. I'm taking this opportunity to express my sincere appreciation to those involved.

First, I would like to express my greatest gratitude to my advisor, Professor Takashi Hirano for all his supports into making this study successful. All the guidance and advices I received were very valuable and thank you for giving me the opportunity to learn. Special thanks also go to Dr. Hiroyuki Yamada for taking care of us in the laboratory. Another important individual that gives countless support is Dr. Ryuichi Hirata. Thank you for allocating your time to provide crucial supports throughout my study period. It is a great honour to work with you.

I also want to thank Prof. Ryusuke Hatano and Prof. Ryoji Sameshima as the examiner for my thesis.

My next gratitude is for Dr. Lulie Melling, the director of Sarawak Tropical Peat Research Institute (STROPI). She gave me the opportunities to engage in this study and continuously gives all the motivational advices. My sincere appreciation also goes to all STROPI staffs that were involved directly or indirectly in this study especially for helping with the field works.

I would like to express my sincere appreciation to both The State Government of Sarawak, The Federal Government of Malaysia and Malaysian Palm Oil Board (MPOB) for funding this research. Thank you for making this research possible and for the continuous efforts into making it run smoothly.

To all the laboratory member of Laboratory of Ecological and Environmental Physics of Hokkaido University School of Agriculture, thank you for all the hospitalities, friendship, and encouragements that you all gave me throughout this study period. All these experiences are priceless and will always be remembered.

I also would like to take this opportunity to thank Japanese Government for the scholarship (Monbukagakusho: MEXT) that provide support for my living in Japan. This is one of the most important support I received to make my study go smoothly.

Last but not least, I would like to thank my family and friends in Sarawak who gave me endless supports and always pray for my wellbeing. To my father, mother, and sisters, I love you all and thank you for the moral support and encouragement. Without you all, any struggles and success will be meaningless.

List of Figures

List of Tables

Table of Contents

Chapter 1: INTRODUCTION

1.1. General

Since the industrial revolution which took place between the 18^{th} to 19^{th} centuries, the usage of fossil fuel had increased in line with the economic development. This was driven by the upsurge in the world population. Fossil fuel includes coal, oil, and natural gas. Energy is extracted from fossil fuel through combustion process, which produces mainly carbon dioxide (CO_2) as its by product as well as other gases such as H_2O, NO_x, and SO_x (where x is the number of oxygen atom). These gases then ended up being deposited into the atmosphere, and eventually disrupt the gases natural composition. These gases are claimed to possess the ability to retain heat in the atmosphere, causing a warming effect known as the "greenhouse effect", hence the name "greenhouse gasses", popularly known as GHGs. Even though the greenhouse effect is essential to the earth to keep its temperature within the habitable spectrum to support life, excessive warming due to GHGs accumulation also could become a threat to living organism. Recently, prolonged human activities have altered the atmospheric GHGs concentration resulting in "excessive" warming, widely known as the "global warming". Global warming is claimed to be responsible in changing both the local and global climatic condition causing the environment to become less and less favourable to all living organisms including human.

CO_2, CH_4, and N_2O altogether account for 80% of total radiative forcing (RF) from well-mixed GHGs. Radiative forcing is the measure of how the energy balance of the Earth-atmosphere system is influenced when factors that affect climate are altered (IPCC, 2007). Radiative forcing is often used to evaluate the influence of a factor that lead to climate change, such as GHGs.

CO_2 is known as the major component of GHGs that gave large impact on global warming. Its atmospheric concentration significantly increased since the early period of Industrial Revolution (1750). Current atmospheric CO_2 concentration is estimated to be ranging from 390.3 to 390.7 ppm in 2011 and this accounts for about 40% increase from that in 1750 (Hartmann *et al.*, 2013). Human activities, changes in land use, and the usage of fossil fuel are claimed to be responsible for the rise (Forster et al., 2007; Hartmann et al. 2013). Since 1750 until 2011, 555±85 PgC were deposited to the atmosphere from anthropogenic CO_2, 375±30 PgC from fossil fuel combustion and cement production, and 180±80 PgC from land use change (France *et al.*, 2013). Significant amount of emitted CO_2 are absorbed by terrestrial ecosystem, hence inferring its strong influence on atmospheric CO_2 concentration (Schimel *et al.*, 2001).

Terrestrial ecosystems stored C in the form of organic compound in living biomass (450-650 PgC) and in the form of dead organic matter in soil and litter (1500-2400 PgC) (Prentice et. al., 2001; Batjes et. al., 1996). The two main components of terrestrial ecosystem CO_2 exchange are the gross primary production (GPP, i.e. photosynthesis) and ecosystem respiration (RE). These processes dominate the carbon (C) balance over a short time period and the balance between these processes are known as the net ecosystem production (NEP).

$$NEP = GPP - RE$$

(Equation 1)

Positive NEP indicates CO_2 absorption by the ecosystem and negative NEP indicates deposition of CO_2 to the atmosphere.

RE comprises autotrophic respiration (RA) from plant and heterotrophic respiration (RH) from animals and microbes.

$$RE = RA + RH$$

(Equation 2)

Plants gain C and energy through GPP, and utilize this energy for growth and cells maintenance before respirate back CO_2 through RA. Therefore, understanding the CO_2 exchange dynamic is vital for understanding the role of terrestrial ecosystem in global C cycle and its importance in regulation atmospheric CO_2 concentration. However, direct measurement of NEP is considered as hard or almost impossible to obtain. The introduction of fast-response CO_2 analyzers and sonic anemometers made it possible to measure net flow of carbon between the ecosystem and atmosphere. Eddy covariance allows instantaneous measurement of gaseous flux over an ecosystem of interest. Net exchange of CO_2 (NEE) between the atmosphere and the ecosystem represent most of CO_2 uptake via GPP and those removed through RE. The term "NEE" was first used by atmospheric scientist community to describe CO_2 deposit to the atmosphere. So, positive NEE indicating CO_2 deposition to the atmosphere (CO_2 source) and negative NEE indicate the otherwise (CO_2 sink). Over a short time period, NEE provides a reasonable estimate of NEP.

$$NEE = -NEP$$

(Equation 3)

NEE may overestimate NEP in terrestrial ecosystem, but it could provide a good illustration for geographic patterns of NEP and its environmental controls (Stuart Chapin *et al.*, 2012).

Large portion of global terrestrial metabolic activity can be traced to tropical forest (Malhi, 2012), which represent about 35% of global NEP (Loescher *et al.*, 2003). Most of intact tropical forests are considered as carbon neutral. However, some early eddy covariance studies, (Song-Miao *et al.*, 1990; Grace *et al.*, 1995) suggested that carbon sequestration occurs in intact old-growth Amazon forests. Despite the sink capacity, representativeness of the current studies of the whole region are still uncertain due to high heterogeneity of the ecosystem and complex meteorology (Schimel *et al.*, 2001). Fan et al. (1990) suggested the possible sensitivity of tropical forests carbon balance to cloud cover and climate fluctuation

(e.g. ENSO). Therefore, more ecosystem scale net carbon exchange study is needed to cover all ecosystem and environmental condition variability.

1.2. Tropical peat swamp forest

Tropical peatlands contain large portion of terrestrial organic carbon (Page et al., 2002). Peatlands are formed through the accumulation of plant and animal residues under waterlogged condition that supress its decomposition (Rydin and Jeglum, 2015). This includes litterfall and dying parts of vegetation below the soil. Living roots, spores, and microbial organisms may also present even in the deep layers but not so dominant. Over 60% of world's tropical peatlands can be found in Southeast Asia and the largest distribution is in Indonesia, with estimated area of 21 Mha or 84% of the total tropical peatlands area, followed by Malaysia (13%, 2–2.5 Mha) and the remainders distributed all over Thailand, Vietnam, Brunei, and the Philippines (UNDP, 2006; Murdiyarso *et al.*, 2010). Koh et. al., (2011) using remote sensing approach estimates large percentage of PSF in Indonesia and Malaysia were converted into OPP, resulting in approximate net biomass C loss of 38 million Mg. Even though the cost for land preparation for converting PSF into OPP are high, as the cost-effective and productive mineral soil become scarcer and the demand for oil palm increase as predicted (Corley and Tinker, 2003), more OPP will be developed on peatlands.

Approximately 11-14% of global peat carbon are located in the tropical region (Page et al., 2011). Large proportion of the total 104.7 Pg tropical peat carbon can be found in southeast Asia (65%, 68.5 Gt), including the newly found peatland in Congo basin (Dargie *et al.*, 2017). Largest distribution of these peatlands is in Indonesia (84%, 21 Mha) followed by Malaysia (13%, 2-2.5 Mha) and the remains scattered all around Thailand, Vietnam, Brunei, and the Philippines (UNDP, 2006; Murdiyarso *et al.*, 2010). Tropical peatlands ecosystems are unique compared to temperate and boreal peatlands due to the coexistence of tropical rainforest and waterlogged woody peat. CO_2 emission from soil are expected to be low under

anoxic condition induced by high groundwater level (GWL), coupled with high biomass productivity made this ecosystem an efficient carbon (C) sink.

1.3. Carbon dioxide emission from tropical peatlands

The massive C stock of tropical peatlands has a high potential to be emitted as CO_2 following land conversion and peat fires (e.g. Hooijer et al., 2012; Miettinen et al., 2017; Jauhiainen et al., 2016a; 2016b; Konecny et al., 2016; Page and Hooijer, 2016), thus transformed it into a net C source. Land conversion in developing countries is usually driven by the needs to grow the economy through agriculture development. The occurrence of peat fires caused by improper land preparation and El Niño events often deteriorate the substantial C emission.

In tropical peatlands, CO_2 emission is reported to be mainly controlled by the local hydrology, due to low variation in soil and air temperature compared to temperate and boreal peatlands. Draining the peatlands deepens the unsaturated peat layer and enhances peat aeration. As a consequent, oxidative peat decomposition theoretically accelerates. This has been proved by previous studies using the eddy covariance technique in tropical peat swamp forest (PSF) in Central Kalimantan (Hirano et al. 2007; 2009; 2012), where high ecosystem-scale CO_2 emission was reported following GWL lowering, attributable to enhanced peat decomposition (Hirano *et al.*, 2014). A study using automated soil chamber system (Sundari et al., 2012) also found a negative relationship between soil respiration (RS) with GWL. However, Hirano et al. (2009) has shown that RE exhibit similar positive relationship with soil temperature as in RS despite the narrow temperature range in the tropic. On the contrary, in an *Acasia* plantation in Indonesia, J. Jauhiainen, Hooijer, & Page, (2012) did not found any significant dependence on temperature using only daytime flux and temperature data. Moreover, Melling et al. (2005) suggested that ecosystem types (e.g. PSF, sago and oil palm plantations) can play important in determining the response of RS to environmental factors,

as they found different main controlling factors for each ecosystem. The heterogeneity of underlying peat in PSF also has a great influence on the vegetation cover, associated with plants adaptation to soil conditions. PSFs are typically formed under ombrotrophic condition and known to have a dome-like shape. Peat depth, peat characteristics and nutrient availability gradually change from the edge to the center of the peat dome. These developed the zonal pattern of PSF known as mixed peat swamp, Alan Batu, Alan Bunga, Padang Alan, Padang Selusor and Padang Keruntum from the edge to the center. PSFs' structure changes from tall and dense to shorter and sparser toward the center (Anderson, 1964; Melling *et al.*, 2007). Similar distinct forest types also found by Page et al. (1999) in Central Kalimantan, Indonesia (mixed peat swamp, low pole, tall interior and very low canopy forests) across the gradient of peat thickness and peat surface elevation. However, the formation of such forest types are more likely determined by the hydrological conditions in relation to mineral and nutrient flows rather than the direct influence of peat thickness and surface topography (Melling *et al.*, 2007).

Published study on the ecosystem-scale CO_2 balance of tropical PSF using the eddy covariance technique are still scarce, currently were limited to Central Kalimantan (Hirano et al., 2007; 2012). Thus, field-derived information is still insufficient. Considering the high heterogeneity of PSF, and high variability in climate (especially precipitation pattern) in tropical regions, more field studies are needed to cover such variability. Therefore, a CO_2 flux study was conducted over a secondary PSF in Sarawak, Malaysia by the eddy covariance technique since 2011. Seasonal variation of precipitation in the study site is less distinct than in Central Kalimantan, and precipitation also less sensitive to ENSO events. Geographically, Sarawak is facing the South China Sea, located in the northwest coast of Borneo Island. This study used four-year-long data from 2011 to 2014 to investigate the environmental dependence of CO_2 fluxes, and the seasonal and interannual variations of CO_2 balance.

Tropical peatlands have been one of the most important arable lands as well as one of the most important resources for Malaysia's economic growth. This is the most accessible arable land with high economic value, but also the least studied and understood soil type in the world. PSF once considered as less valuable for agricultural development owing to its high GWL, high acidity and low fertility. However, with the advancement in scientific and technological knowledge, agricultural activities on tropical peatlands are made possible. Among all crops, oil palm being are regards as the most important strategic crops in Malaysia and Indonesia, the two largest producer of palm oil nowadays. Therefore, more PSF are now converted into large scale oil palm plantation in those countries.

Prior to reclamation, GWL lowering through drainage are crucial to aerate the crop root zone and peat compaction is required to be done to increase the peat soil bulk density, soil surface loadbearing capacity and water-filled pore space (Melling *et al.*, 2005a, 2005b, 2008). However, GWL lowering has been claimed to cause peatlands to shift from C sinks to C sources, increasing CO_2 deposition to the atmosphere, while reducing CH_4 emissions (Furukawa *et al.*, 2005; van Huissteden *et al.*, 2006; Couwenberg, 2011). This is associated with enhanced microbial degradation of organic matter in soil that increased decomposition rate of peat as observed in boreal and temperate peatlands. However, this is not necessary applicable to topical peatland due to the differences in peat soil properties, environmental factors, microbial community, vegetation and management practices. To date, published data on ecosystem scale CO_2 fluxes after PSF conversion to oil palm plantation (OPP) are nonexistence. This study focussed to study CO_2 dynamic in former PSF after conversion, investigate the main controlling factors of CO_2 fluxes, and assessed the seasonal and inter-annual variation of the fluxes.

1.4. Objectives

This study was conducted with the following objectives; a) Assess the seasonal and interannual variations of the CO_2 balance in a peat swamp forest (PSF) and an oil palm plantation (OPP) on peat, b) Investigate the main environmental controls of CO_2 fluxes in both ecosystems and c) Assess the effect of PSF conversion to OPP and explore possible CO_2 emission reduction strategy.

Chapter 2: MATERIALS AND METHODS

2.1. Study site

The study sites were located at the state of Sarawak, Malaysia, in the Island of Borneo (**Figure 1**). The OPP site was about 100 km away from the PSF site. PSF was used to represent the condition before conversion and OPP represent condition after conversion. The climate in this region is mainly influenced by the Northeast and Southwest monsoon (Malaysian Meteorological Department, 2013). Monsoon occurs when there is a temperature difference between the lands and sea, induced by the solar radiation. The Southwest monsoon generally begins in late May until September and Northeast monsoon from November to March. The Southwest monsoon bring relatively drier weather, while the Northeast monsoon bring heavy rainfall especially to the western part of Sarawak.

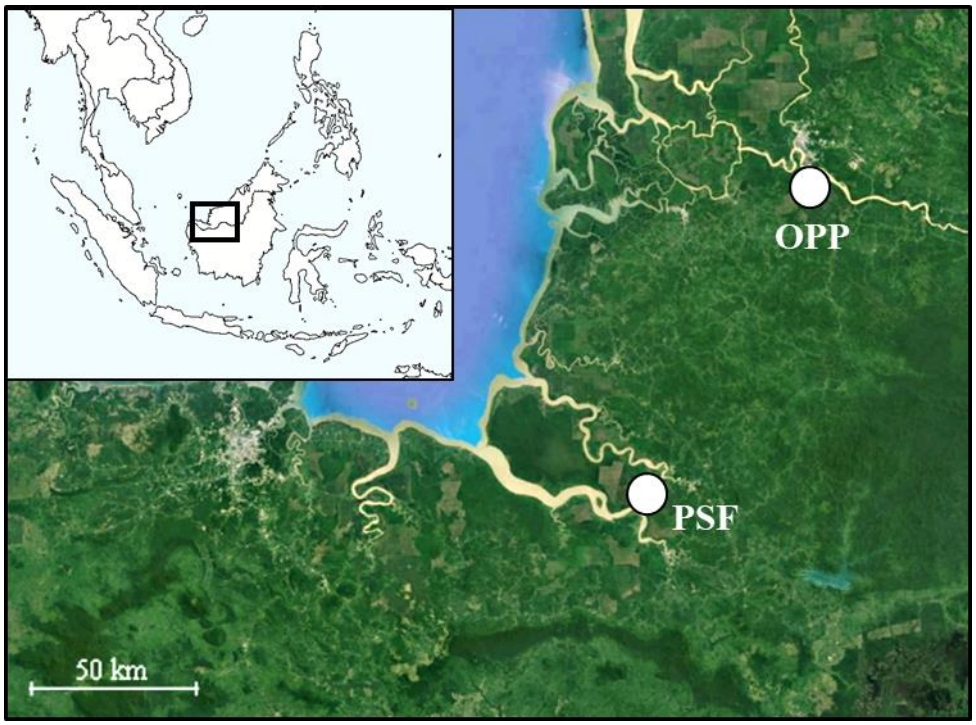

Figure 1. Study sites location in Sarawak, Malaysia (Source: Google maps).

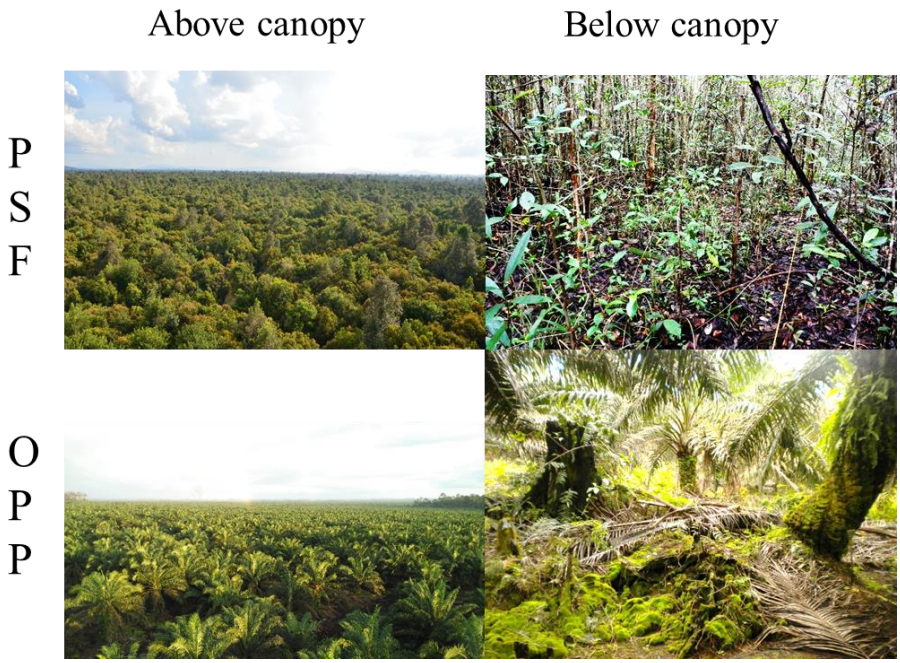

Figure 2. *Above and below canopy views in PSF and OPP.*

PSF used for this study is located in Betong division of Sarawak, Malaysia. An eddy covariance tower with the height of 40 m was constructed inside the 25.6 km^2 forest, around the center (1°23'59.42"N, 111°24'6.69"E) of a peat dome. Satellite estimated elevation of the area was about 17 m a.s.l., with an almost flat terrain. Peat at the tower site accumulated up to 10 m depth above the substratum. The forest regenerated into a secondary forest after experienced selective logging. Logging in the windward area (southeast direction from the tower) was almost terminated in 1980s, and the surrounding area of the forest was converted into oil palm plantations in 1990s. The forest type at the tower site is described as the transition between Alan Bunga and Padang Alan forests. Originally, the forest was dominated by *Litsea* spp., but recently has been outgrew by original trees species known as *Shorea albida*. In 2016, the tree density was estimated at 1990 trees ha^{-1}. During the beginning of flux measurement in 2010 the canopy height was about 25 m. Plant area index (PAI) was not measured until 2013. Average PAI obtained monthly using a plant canopy analyser (LAI2000, Li-Cor Inc., Lincoln, NE, USA) was 7.9 m^2 m^{-2} from April 2013 to March 2014; with no clear seasonal variation. Typical hummocks and hollows microtopography are present on the

forest floor, with significant accumulation of leaf. Saplings are also abundant below the canopy. Melling, (2013) described the physical and chemical properties of peat soil at this site (abbreviated as CA).

CO_2 flux was measured in an oil palm plantation located in Sibu division of Sarawak, Malaysia (02º11'12"N, 111°50'35.7"E), where an eddy covariance tower with the height of 41 m was constructed. In September 2004, the former mixed peat swamp forest with total area about 10, 000 ha was developed into an oil palm plantation. The current peat thickness was between 8-11 m (Sangok et al., 2017). *Elaeis guineensis* was planted with planting density of 153 trees ha^{-1}. During the beginning of flux measurement in 2011, the oil palm trees in the EC footprint area was aged between 3 to 7 years old with the approximate average height of 8 m. Plant area index (PAI) was averaged at 3.73 m^2 m^{-2} (October 2013 to December 2014). Understorey was dominated by fern (*Stenochlaena palustris* (Burm. f.) Bedd.). During harvesting the lowest fronds were cut and gathered in row causing leaf litter accumulation on the ground. Large tree stumps leftover from land clearing also abundant on the ground. Considering the common practice of replanting every 25-30 years, the study site in the first cycle of cultivation. Ditches were excavated, and water gates installed to control the GWL at roughly -60 cm, as one of the management practice for better palm growth, preventing peat fires, and reducing peat decomposition by reducing aerated zone in the top soil. Fluxes and micrometeorological measurements were similar to those in PSF.s

2.2.Flux measurement

NEE was obtained by adding CO_2 flux above the canopy to the CO_2 storage change below the canopy (NEE = CO_2 flux + CO_2 storage change). CO_2 flux (F_C) was determined from CO_2 concentration fluctuation (c') measured using an open-path CO_2/H_2O analyzer (LI7500A, Li-Cor Inc.) and vertical wind velocity fluctuation (w') measured using a sonic

anemometer/thermometer (CSAT3, Campbell Scientific Inc., Logan, UT, USA). Instrumentations for flux measurement are shown in **Figure 3**.

$$F_C = \overline{w'c'}$$

(Equation 4)

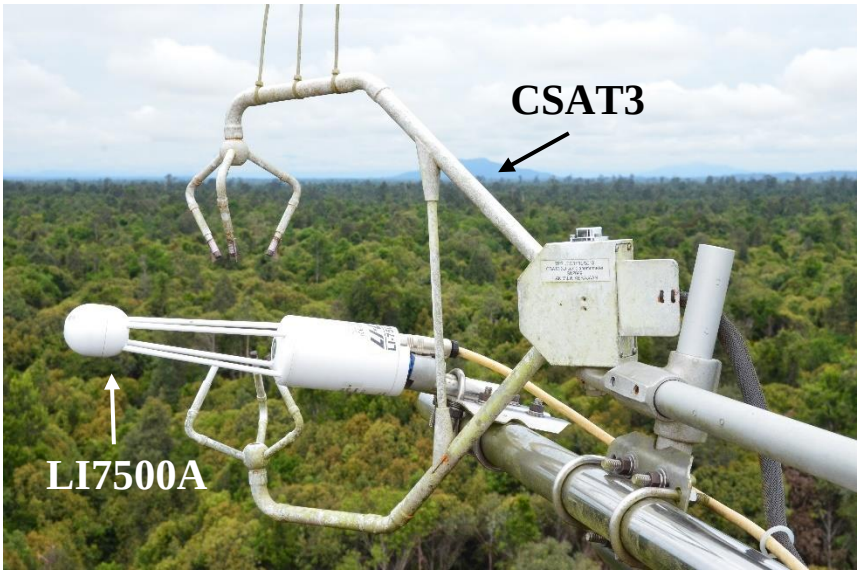

Figure 3. *open-path CO_2/H_2O analyzer (LI7500A, Li-Cor Inc.) and a sonic anemometer/thermometer (CSAT3, Campbell Scientific Inc., Logan, UT, USA).*

At both forest and oil palm plantation, CO_2 and energy fluxes have been measured at the height of 41 and 21 m respectively using the EC technique since October 2010. The flux measurement heights (h_m) were determined by considering the height of vegetation (h_c) to ensure sensors were placed right on top of the surrounding canopy in the well-mixed surface layer and avoid disproportionate height that can extend the footprint beyond the boundary layer under calm night-time condition. The following equation was used to estimate h_m:

$$h_m \approx d + 4(h_c - d)$$

where d is the zero-plane displacement (d=2/3 h_c).

Measurement heights (m)	
PSF	OPP
41	21
21	11
11	5
3	3
1	1
0.5	0.5

Table 1. *Measurement heights for CO_2 profile in PSF and OPP.*

CO_2 storage change (F_C) are almost negligible over short vegetation but can become significantly large over high canopy like forest. Thus, it should be considered in NEE calculation. Temporal change of the atmospheric CO_2 concentration below the flux measurement are used for F_C evaluation. CO_2 profile was measured at multiple heights considering the unequal vertical distribution of CO_2 concentration below the canopy. Eventually, F_C was calculated from CO_2 profile measurements at 6 heights (**Table 1**) using the following equation:

$$F_S = \int_0^{h_m} \overline{\frac{\partial \rho_c}{\partial t}}\, h$$

(Equation 5)

Where, F_S: CO_2 storage change [mg m^{-2} s^{-1}], ρ_c: CO_2 concentration [mgm^{-3}], t: time (s), h: height [m], and h_m: flux measurement height [m].

Positive NEE indicates that the ecosystem is a net CO_2 source, whereas negative NEE indicating a net CO_2 sink.

CO_2 and energy fluxes have been measured since October 2010 at the height of 41 m using the eddy covariance technique, but only data from January 2011 to December 2014 will be used for analysis. Three-dimensional wind velocity, air temperature, CO_2 density and water vapor density were measured using a sonic anemometer/thermometer (CSAT3, Campbell Scientific Inc., Logan, UT, USA) and an open-path CO_2/H_2O analyzer (LI7500A, Li-Cor Inc.) at 10 Hz frequency. CO_2 concentrations were also measured every minute rotationally at the heights of 41, 21, 11, 3, 1, and 0.5 m using a closed-path CO_2 analyzer (LI-820, Li-Cor Inc.). Raw data were recorded with a data logger (CR3000, Campbell Scientific Inc.).

Half-hourly mean CO_2 flux (F_C) was calculated from raw eddy data using a software, Flux Calculator (Ueyama *et al.*, 2012). Through the calculation, spike removal (Vickers and Mahrt, 1997), planar fit rotation (Wilczak *et al.*, 2001), frequency response correction (Massman, 2000) and air density fluctuation correction (Webb *et al.*, 1980) were applied. CO_2 storage below the flux measurement height was estimated at intervals of 5 min from CO_2 concentrations measured at the six heights (*Section 2.2*) by temporal linear interpolation (Hirano et al., 2007). Then, we calculated half-hourly CO_2 storage flux (F_S) as the change of CO_2 storage. Finally, the net ecosystem exchange (NEE) of CO_2 was calculated as the sum of F_C and F_S (NEE = F_C + F_S). Positive NEE indicates that the ecosystem is a net CO_2 source, whereas negative NEE indicating a net CO_2 sink.

2.3.Meteorological measurements

Global and reflected solar radiations and long-wave radiations (upward and downward) were measured using a radiometer (CNR4, Kipp&Zonen, Delft, the Netherlands) at the height of 41 m. Downward and upward photosynthetic photon flux densities (PPFD) were also measured at the same height using two quantum sensors (LI-190, Li-Cor Inc.). Wind speed and direction were measured with a vane and three-cup anemometer (Wind

sentry, Young, Traverse City, MI, USA) at the height of 41m. Air temperature (T_a) and relative humidity (RH) were measured with a temperature & relative humidity probe (CS215, Campbell Scientific Inc.) in a radiation shield (41303-5A, Campbell Scientific Inc.) at the heights of 11 and 41 m, respectively. Water vapor pressure deficit (VPD) was calculated from T_a and RH. GWL was measured at one point with a water level logger (STS DN/L 50, Sensor Technik Sirnach AG, Danbury, CT, USA); GWL was the distance between the groundwater surface and the ground surface at a hollow. Volumetric soil water content (VWC) was measured in the uppermost 30-cm-thick layer at a hollow using a TDR sensor (CS615, Campbell Scientific Inc.). Soil temperature (T_s) was measured using resistance thermometers at 5 and 10 cm depths, respectively. Precipitation (PT) was measured using a tipping-bucket rain gauge (TE525, Campbell Scientific Inc.) at the height of 1 m in an open space close to the tower. These data were averaged and recorded half-hourly using a datalogger (CR3000, Campbell Scientific Inc.).

The measurement was occasionally interrupted mainly because of power problems. The resultant data gaps in PPFD, T_a and VPD were filled by linear regression with data measured on a tower (1°27'55"N, 111°09'20"E) in another PSF site, about 20 km away from this site. Missing PT was filled on a daily basis with data of a nearby meteorological station (Lingga) about 26 km away; root mean square errors (RMSEs) were 11 mm day-1 and 51 mm month^{-1}, respectively, on daily and monthly bases. Missing GWL was estimated hydrologically by the tank model method (Sugawara, 1979).

2.4. Quality control, gap filling and partitioning of NEE

Prior to gap-filling, NEE data were screened by the mean absolute deviation (MAD) spike detection method (Papale *et al.*, 2006) and the deviation of each half-hourly NEE from mean diurnal variation (MDV). MDV and standard deviation (SD) were calculated for a 14-day-long moving window. If NEE was out of 3 SDs ± MDV, it was removed. NEE under low

turbulent conditions during the nighttime (PPFD ≤ 10 μmol m^{-2} s^{-1}) was filtered using a friction velocity (*u**) threshold determined using Flux Analysis Tool software (Ueyama *et al.*, 2012); the *u** threshold was determined at 0.15 m s^{-1} at this site. Finally, the gaps were filled using the marginal distribution sampling (MDS) method (Reichstein et al., 2005). The size of moving windows was between 7 and 49 days depending on the length of data gaps and the availability of "look up" values. We performed gap filling separately for the daytime (PPFD > 10 μmol m^{-2} s^{-1}) and the nighttime (PPFD ≤ 10 μmol m^{-2} s^{-1}). Following a flux study in PSFs (Hirano et al., 2012), PPFD, VPD and T_a were used during the daytime, whereas GWL, T_s and VWC were used during the nighttime. Missing NEE was "looked up" based on similar environmental conditions of ± 25 μmol m^{-2} s^{-1} for PPFD, 0.15 kPa for VPD, 2.5 cm for GWL, 0.05 m^3 m^{-3} for VWC, 1.0°C for T_a and 0.2°C for T_s. Daytime ecosystem respiration (RE) was "looked up" from nighttime NEE using the same algorithm for gap-filling (MDS). Then, gross primary production (GPP) was calculated as the difference between NEE and RE (NEE = RE – GPP). During the nighttime, GPP was set to zero.

2.5.Light response parameters of NEE

Ecosystem photosynthetic parameters were calculated by fitting a non-rectangular hyperbola function (エラー! 参照元が見つかりません。) to measured PPFD and daytime NEE.

$$\mathrm{NEE} = -\frac{1}{2\theta}\left(\alpha\, PPFD + P_{max} - \sqrt{(\alpha\, PPFD + P_{max})^2 - 4\alpha\, P_{max}\, \theta\, PPFD}\right) + RE_d$$

(Equation 6)

where θ is the curvature (set to be 0.9), α is the initial slope, P_{max} is the maximum GPP, and RE_d is the dark respiration. Fitting was conducted on a daily basi. The photosynthetic parameter P_{max} was assessed for seasonality together with GPP.

2.6.Definition of the wet and dry periods

Data in PSF forest ware grouped into wet and dry period using the following procedure. The driest month with the least PT generally occurs in June or July in this area (Fig. 1a). In the tropics, a threshold of monthly PT < 100 mm is commonly used to determine the dry season (Malhi *et al.*, 2002). According to this threshold, the dry season was very short in this site, because monthly PT barely dropped below 100 mm. Thus, to extract a relatively dry period, we analysed monthly PT using 15-year-long data at Lingga meteorological station (as mentioned above). As a result, the median of monthly PT (238 mm) was used to separate the relatively dry period and the wet period. The durations of each period are shown in Table 1. Conventionally, a hydrological year was determined to be from the onset of a dry period to the end of the next wet period. According to the PT threshold, the onset of the dry period shifted year by year (**Table 3**). The hydrological years were named Y1, Y2, Y3 and Y4, respectively, during the duration from April 2011 to September 2014 (**Figure 7**a and **Table 3**).

2.7.Statistical analysis

The means of NEE, RE, GPP and environmental factors were compared between the dry and wet periods by t-test. Those of each period were compared by Tukey's HSD. Regression coefficients of light-saturated NEE with VPD were compared between the two periods by t-test. These analyses were performed using R version 3.3.1 software.

2.8.Aboveground Biomass estimation

Aboveground biomass (AGB) estimation was estimated using different method for both PSF and OPP.

In the PSF, AGB was estimated following allometric equations developed by Monda et. al, (2015), established specifically for PSF by considering the hollows inside the tree trunk. The allometric equation is as follow:

$$AGB\ (kg) = \exp(-3.5339 + 3.7146 \ln(DBH) - 0.2529 [\ln(DBH)]\ 2) \quad \text{(Equation 7)}$$

Biomass was assumed to contain 50% carbon (C).

In the forest, four tree inventory plots (30 m x 40 m for each plot) were set up with overall 16 plots shown in **Figure 5**. Trees with DBH (diameter at breast height) greater than 5cm were selected and measured. The locations and coordinates of the plots are shown in **Figure 4** and **Table *2***. In order to improve the measurement precision, the "breast height" need to be standardized. The height of 1.3 m above ground was selected in accordance with the international practice.

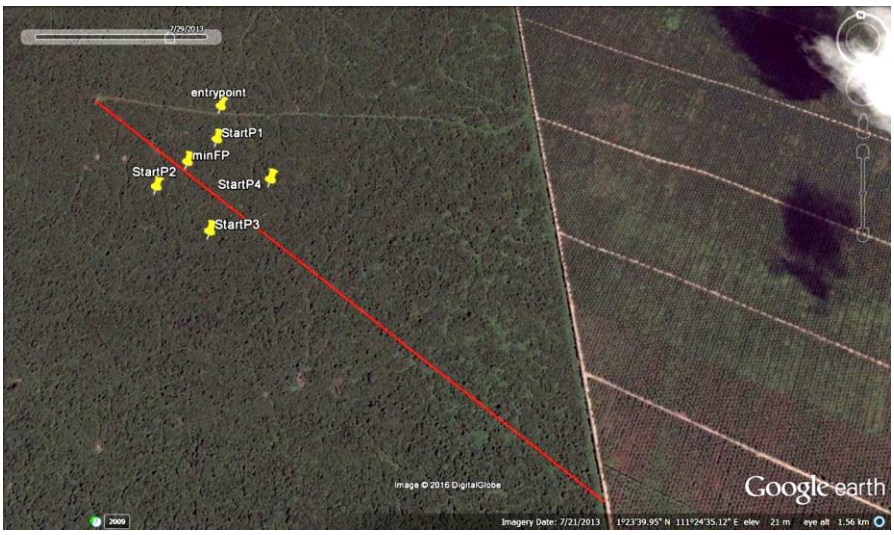

Figure 4. *Location of tree inventory plots (source: Google earth).*

Plot No.	Coordinates
StartP1	N 1^0 23' 53.20'' E 111^0 24' 16.87''
StartP2	N 1^0 23' 48.62'' E 111^0 24' 12.28''
StartP3	N 1^0 23' 43.05'' E 111^0 24' 17.80''
StartP4	N 1^0 23' 47.70'' E 111^0 24' 22.40''

Table 2. *Coordinates for Tree inventory plots in PSF.*

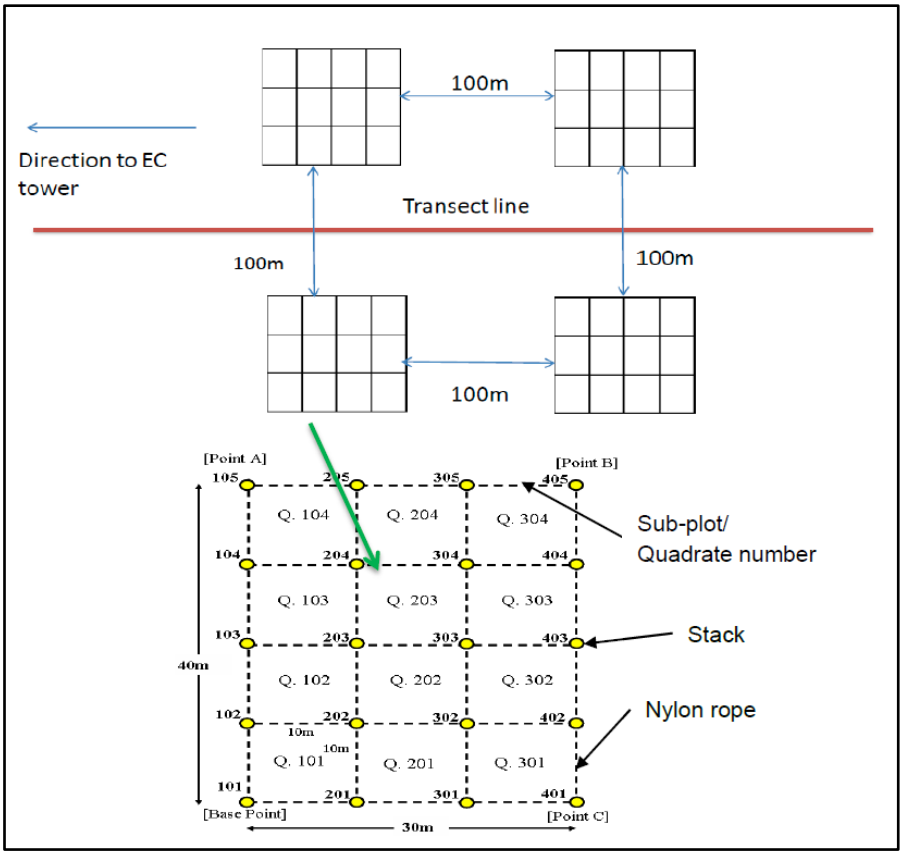

Figure 5. *Tree inventory plot for PSF site.*

DBH measurement can be tricky in the case where tree's shape is unusual. Trees with criteria listed below are excluded:

1) Presence of fork below breast height

2) Trees splitting into several stem

3) Leaning trees

Sometimes, buttress of the trees can extend beyond the DBH measurement height (>1.3 m). in this case, the diameter was taken just above the buttress (**Figure 6**).

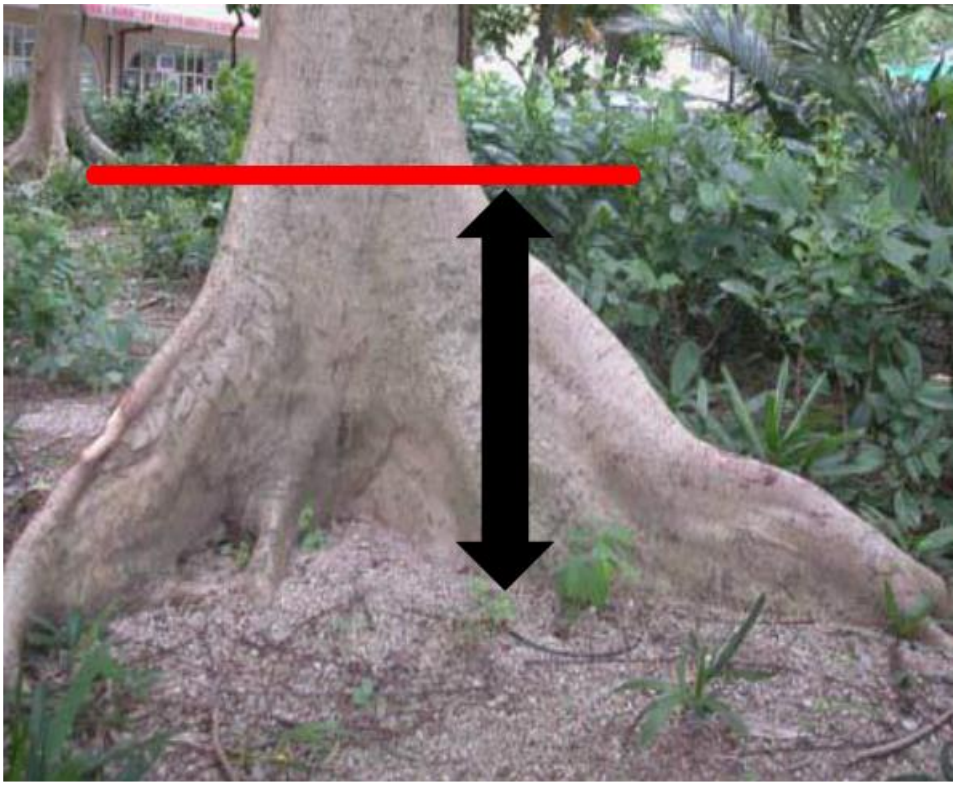

Figure 6. *DBH measurement for trees with buttress higher than 1.3 m above the ground. Red line indicates the alternative "breast height".*

At the OPP, only tree height measurement was used for AGB estimation, using equation developed by Khasanah et. al., (2015).

Chapter 3: CARBON DIOXIDE FLUXES OVER A SECONDARY PEAT SWAMP FOREST

3.1. Results

3.1.1. Environmental conditions

Seasonality in PT was partly attributable to ENSO events; a La Niña event occurred from 2010 to early 2012, and weak El Niño events occurred in 2012 and 2014, which are determined by sea surface temperature (SST) anomalies (http://www.cpc.ncep.noaa.gov/). The longest wet period was in Y1 (8 months) in relation to a La Niña event, and the dry period was longest in Y3 (8 months) (**Table 3**). The driest month (monthly PT < 100mm) was generally recorded in June or July, whereas it occurred also in February in 2014 (**Figure 7**a). Cumulative PT in the dry periods accounted for 22.1, 43.5, 43.7 and 61.2% of total PT in Y1, Y2, Y3 and Y4, respectively, whereas mean monthly PT was significantly lower in the dry period (**Table 3**). Annual PTs on a calendar basis in 2011, 2012, 2013 and 2014 were 2965, 2729, 2563 and 2120 mm, respectively (**Table 5**). Following the seasonality of PT, GWL decreased in the dry period (**Figure 7**b). On average, GWL was -9 cm in the wet period and -29 cm in the dry period (**Table 3**). During the wet period in 2011 (W1), GWL rose up to 30 cm aboveground, but only for a short period. In this site, however, flooding was uncommon even during the wet period. The lowest GWL of -67 cm was recorded in the 2011 dry period (D1). Correspondingly, VWC was significantly lower during the dry period (p < 0.01, **Table 3**).

Daily PPFD was significantly lower by 6% during the wet period (p < 0.01, Table 2) following the increase in PT (**Figure 7**a and **Table 3**). The lowest daily PPFD was recorded in the W2 (32.6 mol m^{-2} day-1), and the highest was in the D1 and D2 (35.8 mol m^{-2} day-1, **Table 3**). Annual PPFD in 2011, 2012, and 2014 was the same at 12.5 kmol m^{-2} year-1, but

increased slightly to 12.8 kmol m^{-2} year-1 in 2013 (**Table 5**). Daily mean T_a at the height of 41 m fluctuated between 23 and 30ºC (**Figure 7**d). Daily minimum and maximum T_a ranged from 19.8 to 25.9 ºC and from 24.5 to 35.5ºC, respectively (data not shown). Mean T_a was significantly higher in the dry period ($p < 0.01$), but the difference was small (0.7ºC, **Table 3**). Both daily minimum and maximum T_a increased in the dry period similarly to daily mean T_a. Annual mean T_a was almost constant between 26.4 and 26.6ºC. Daily mean T_s increased linearly with daily mean T_a (data not shown). Daytime VPD was also significantly higher in the dry period (**Table 3**), probably owing to increased T_a. The lowest VPD was generally recorded in early-January and gradually increased to its peak in late June (**Figure 7**e). Daytime VPDs during D1 and D2 were significantly higher than those in the other dry periods (**Table 3**).

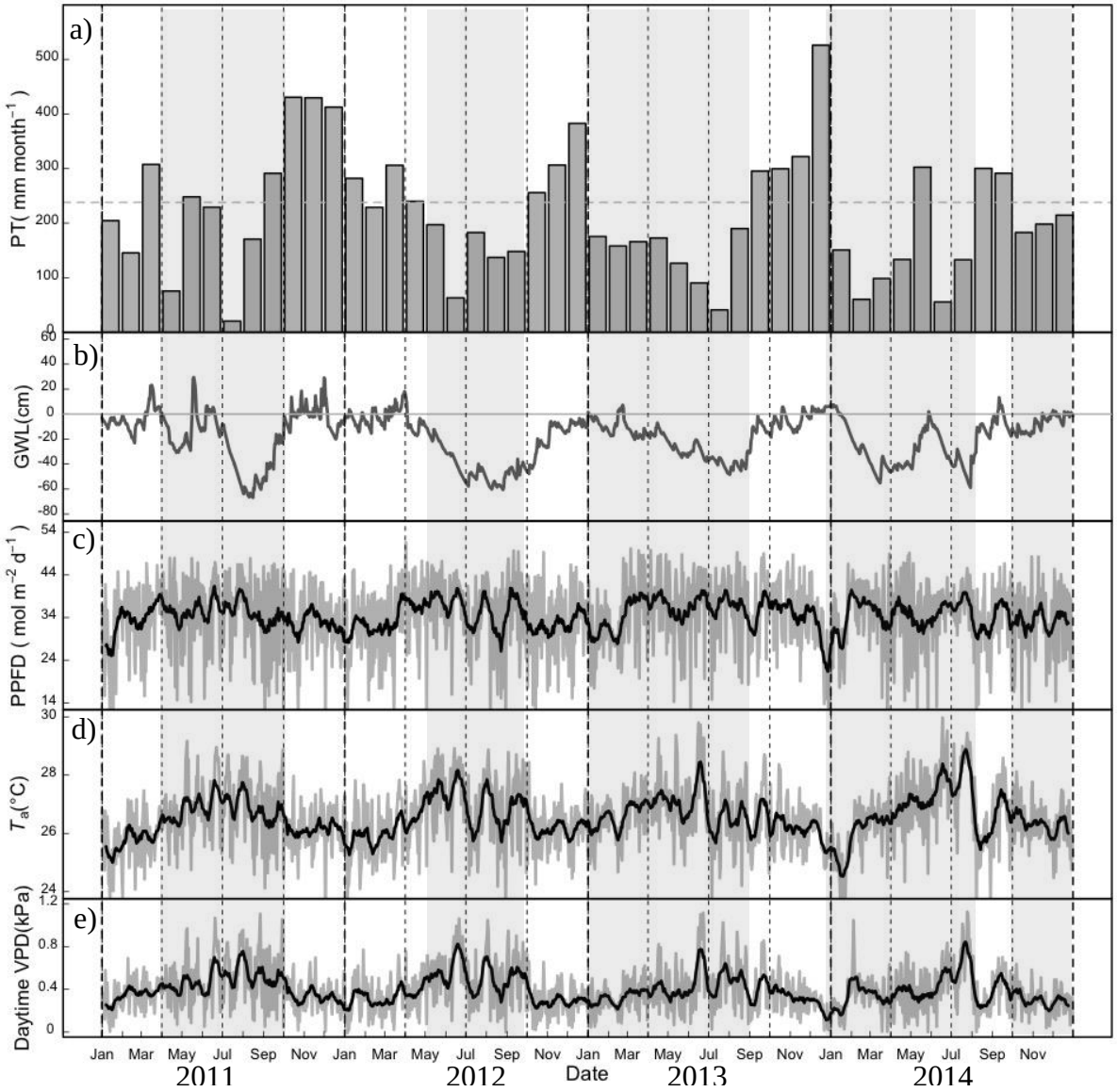

Figure 7. *Seasonal variations of monthly precipitation (PT) (a), daily mean groundwater level (GWL) (b), daily photosynthetic photon flux density (PPFD) (c), daily mean air temperature (T_a) (d) and daytime mean vapor pressure deficit (VPD) (e) from January 2011 to December 2014. Black lines are 14-day-long moving averages. Bold dashed vertical lines are the border of calendar years. The horizontal dotted line in (a) is the median of 15-year-long PT data measured at Lingga station. Grey areas denote the dry periods.*

3.1.2. Seasonality of CO_2 fluxes

Seasonal variations in daily NEE, RE and GPP are shown in **Figure 10**. In general, daily NEE was more positive in the dry periods and became slightly neutral or more negative in the wet periods (**Table 4**). Daily RE varied similarly with NEE. The variation of daily GPP was smaller than RE. Daily NEE and RE were significantly different between the two periods ($p < 0.01$), respectively, whereas no significant difference was found in daily GPP ($p > 0.05$) (Table 2). As a result, the seasonal difference in NEE (0.52 g C m^{-2} day-1) was due to RE (0.57 g C m^{-2} day-1).

3.1.3. Controlling factors of CO_2 fluxes

In order to investigate the response of RE to environmental conditions, measured NEE (RE) was plotted against GWL and VWC. Nighttime NEE increased significantly as GWL (r = -0.53, p = 0.01) or VWC (r = -0.42, p = 0.04) lowered (**Figure 8**). According to the relationship, RE increased linearly by 0.28 μmol m^{-2} s^{-1} for every 10 cm lowering in GWL, and RE was 8.5 μmol m^{-2} s^{-1} when GWL was 0 cm.

Photosynthetic response was analyzed using light-saturated NEE (PPFD > 1000 μmol m^{-2} s^{-1}) instead of GPP to avoid uncertainties caused by flux partitioning procedures. Figure 3 shows the response of light-saturated NEE to VPD in the dry and wet periods. Light-saturated NEE showed a positive relationship with VPD ($p < 0.01$) in both periods; there was no significant difference in the regression coefficients between the two periods ($p > 0.05$). Means (± 1 SD) of light-saturated NEE in the dry and wet periods were -18.2 ± 9.0 and -19.1 ± 9.0 μmol m^{-2} s^{-1}, respectively. Maximum GPP (P_{max}) was 33.7 and 34.1 μmol m^{-2} s^{-1}, respectively, on average in the dry and wet periods (**Table 4**); these were not significantly different.

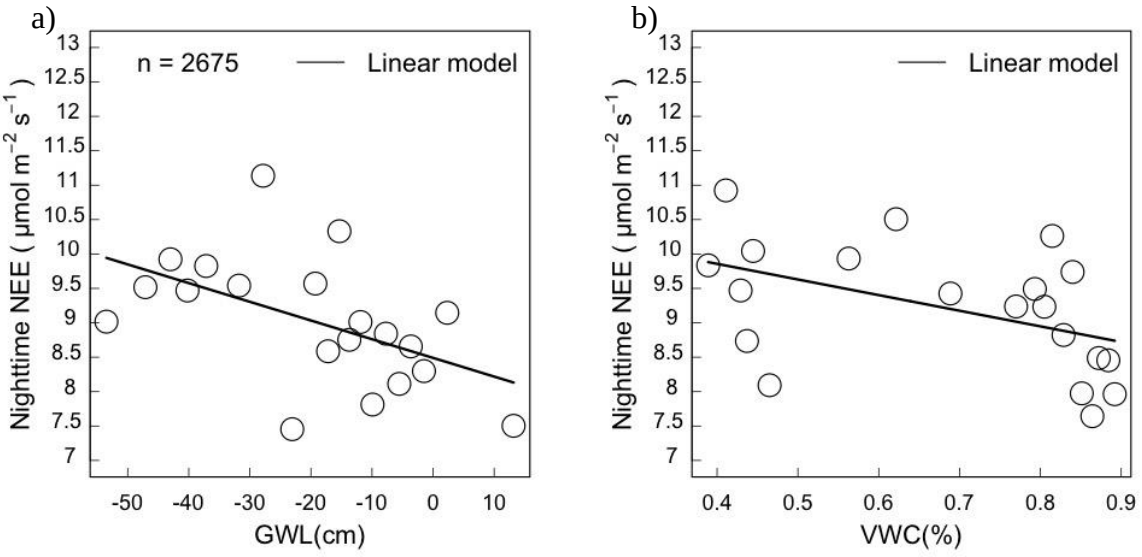

Figure 8. Relationship between measured nighttime NEE and groundwater level (GWL) (a) or soil water content (VWC) (b). Half-hourly NEE data were sorted according to GWL or VWC and bin-averaged for 20 classes in the same size. Lines were drawn for significant relationship ($p < 0.05$).

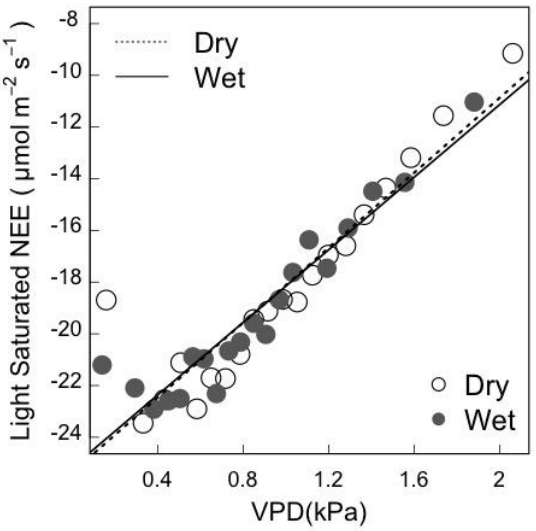

Figure 9. *Response of NEE to vapor pressure deficit (VPD) in light-saturated conditions (PPFD > 1000 µmol m^{-2} s^{-1}). Half-hourly measured NEE was plotted against VPD separately for the dry and wet periods. NEE data were sorted according to VPD and binned into 20 classes in the same size. Lines were drawn for significant relationship (*$p < 0.01$*).*

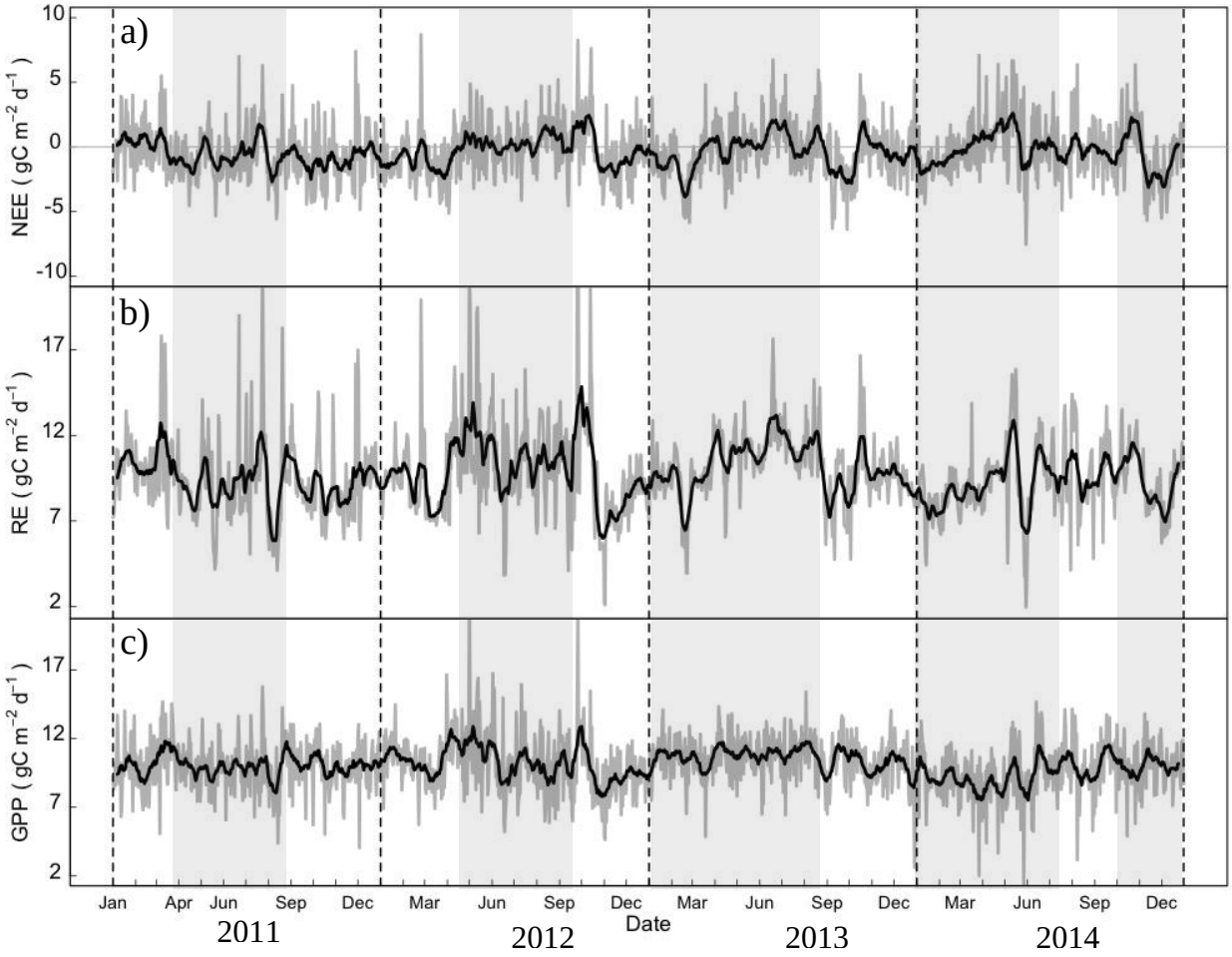

Figure 10. *Seasonal variation in daily values of NEE (a), RE (b) and GPP (c) from January 2011 to December 2014 (grey lines) after gap-filling. Black lines are 14-day-long moving averages. Grey shades indicate the dry periods. Dotted vertical lines are the calendar year border.*

3.1.4. Aboveground Biomass

Tree inventory for AGB study in PSF site only started in 2016 and conducted on annual basis. In 2016, AGB was estimated at 140 t ha^{-1} (7000 g C m^{-2} year^{-1}). AGB increased to 145.8 t ha^{-1} (7292 g C m^{-2} year^{-1}) in 2017.

3.1.5. Annual CO_2 balance

Four-year-mean of annual NEE was -136 ± 51 g C m^{-2} year-1 (mean ± 1 SD), ranged from -207 (2011) to -98 g C m^{-2} year-1 (2012), resulting from GPP of 3682 ± 149 g C m^{-2} year-1 and RE of 3546 ± 149 g C m^{-2} year-1 (**Table 5**). The highest and lowest annual RE and GPP occurred in 2013 and 2014, respectively. The rank orders of NEE and RE or GPP

were inconsistent. Annual NEE was negatively correlated with annual mean of GWL (r = -0.92, data not shown), but it was not significant (p = 0.08) because of a small sample size (n = 4). There was no significant relationship between RE and GPP with GWL (r = -0.14 and 0.17, respectively). The relationship between annual fluxes (NEE, RE, and GPP) with PT or PPFD was weak ($r^2 < 0.49$).

Table 3. *Duration of the wet and dry periods from 2011 to 2014. Duration between the onset of a dry period and the end of the subsequent wet period was defined as one hydrological year named as Y1, Y2, Y3 and Y4, respectively.*

Year	Period	Duration	Length (Months)
2011 – 2012 (Y1)	Dry (D1)	April 2011 – August 2011	5
	Wet (W1)	September 2011 – April 2012	8
2012 – 2012 (Y2)	Dry (D2)	May 2012 – September 2012	5
	Wet (W2)	October 2012 – December 2012	3
2013 – 2013 (Y3)	Dry (D3)	January 2013 – August 2013	8
	Wet (W3)	September 2013 – December 2013	4
2014 – 2014 (Y4)	Dry (D4)	January 2014 – July 2014	7
	Wet (W4)	August 2014 – September 2014	2

Table 4. *Means of daily CO_2 fluxes and environmental variables in each period (mean ± 1 standard deviation (SD)).*

Period	NEE (g C m^{-2} day^{-1})	RE (g C m^{-2} day^{-1})	GPP (g C m^{-2} day^{-1})	P_{max} (μmol m^{-2} s^{-1})	PPFD (mol m^{-2} day^{-1})	Daytime VPD (kPa)	T_a (°C)	VWC (m^3 m^{-3})	GWL (cm)	PT (mm $month^{-1}$)
D1	-0.76 ± 2.04bc	9.09 ± 2.75b	9.85 ± 1.84bc	33.2 ± 9.7ab	35.8 ± 8.0a	0.77 ± 0.31a	26.9 ± 1.0a	-	-27.6 ± 22.9de	149 ± 98
D2	0.40 ± 2.06a	10.85 ± 3.38a	10.45 ± 2.74ab	35.6 ± 9.7ab	35.8 ± 8.4a	0.81 ± 0.34a	27.0 ± 1.2a	0.50 ± 0.14e	-41.5 ± 13.7f	146 ± 52
D3	-0.23 ± 2.09abc	10.53 ± 1.94a	10.76 ± 1.52a	33.5 ± 9.8ab	35.7 ± 8.0a	0.67 ± 0.30b	26.8 ± 1.0ab	0.69 ± 0.15c	-23.0 ± 13.5cd	140 ± 51
D4	-0.14 ± 2.24ab	9.10 ± 2.13b	9.24 ± 1.96c	32.8 ± 10.6a	35.1 ± 7.9ab	0.63 ± 0.28bc	26.8 ± 1.3ab	0.62 ± 0.18d	-28.6 ± 16.8e	133 ± 83
W1	-0.92 ± 2.05c	9.39 ± 2.14b	10.30 ± 1.68ab	33.3 ± 9.3ab	33.2 ± 8.5b	0.62 ± 0.29bcd	26.2 ± 1.0c	-	-6.3 ± 14.0a	328 ± 84
W2	-0.49 ± 2.26bc	8.81 ± 2.78b	9.30 ± 1.86c	31.8 ± 8.7b	32.6 ± 8.2b	0.52 ± 0.24d	26.2 ± 0.7c	0.74 ± 0.13bc	-17.5 ± 12.5bc	315 ± 64
W3	-0.70 ± 2.19bc	9.42 ± 1.80b	10.12 ± 1.75ab	37.1 ± 11.1a	33.9 ± 8.1ab	0.57 ± 0.26cd	26.2 ± 0.9c	0.83 ± 0.07a	-5.3 ± 8.0a	361 ± 111
W4	-0.21 ± 1.84abc	9.81 ± 2.11ab	10.02 ± 2.12abc	34.6 ± 12.4ab	33.2 ± 8.0b	0.53 ± 0.24cd	26.4 ± 1.2bc	0.81 ± 0.11ab	-11.1 ± 11.3ab	296 ± 6
Dry	-0.18	9.91	10.09	33.7	35.5	0.71	26.9	0.62	-29.2	141
Wet	-0.71	9.34	10.05	34.1	33.3	0.58	26.2	0.82	-8.6	329
Sig. (t-test)	***	***	*NS*	*NS*	***	***	***	***	***	***

Values marked with the different letter in each column are significantly different ($p < 0.05$) according to Tukey's HSD test. As for seasonal means, t-test was applied (***: $p < 0.01$). *NS* indicates no significant different between seasons.

Table 5. *Annual CO_2 balance and annual mean of environmental variables from 2011 to 2014 on a calendar basis in PSF.*

Year	NEE	RE	GPP	PPFD	GWL	PT
		(g C m^{-2})		(kmol m^{-2})	(cm)	(mm)
2011	-207	3450	3657	12.5	-15.7	2965
2012	-98	3633	3731	12.5	-22.8	2729
2013	-140	3708	3848	12.8	-17.1	2563
2014	-100	3392	3492	12.5	-20.3	2120
Mean ± SD	-136 ± 51	3546 ± 149	3682 ± 149	12.6 ± 0.2	-19.0 ± 3.2	2594 ± 356

3.2. Discussion

Seasonal variation in PT was not so clear in this study site during the four years. Only one or two dry months defined as monthly PT less than 100 mm appeared per calendar year (**Figure 7**a). Thus, the relatively dry period and the wet period were differentiated using median (238 mm) of monthly PT from 15-year-long data recorded at a nearby meteorological station. As a result, daily NEE was significantly less negative in the dry period than in the wet period (**Table 4**). The seasonal difference of NEE between the dry and wet periods was 0.53 g C m^{-2} day-1 on average, which was almost equivalent to that of RE (0.57 g C m^{-2} day-1). Daily RE was significantly greater in the dry period mainly because of lower GWL or VWC (Fig. 2). Lower GWL enhances peat aeration and potentially increases oxidative peat decomposition, which results in higher soil CO_2 efflux (e.g. Hirano et al., 2012, 2014). In contrast, daily GPP showed no significant seasonal differences (**Table 4**) probably because of compensation effects between PPFD and VPD. In the wet period, although lower PPFD decreased GPP, lower daytime VPD eased the reduction in light-saturated NEE due to stomatal closure (Fig. 3). Also, maximum GPP (P_{max}) showed no significant seasonal difference (**Table 4**). Moreover, plant area index (PAI) showed no seasonal variation. These results suggest that the fluctuation in GWL between 0 and -60 cm did not influence the photosynthetic parameters of this ecosystem. A study in Amazonian rainforest by Goulden et al. (2004) found a reduction in photosynthesis which started right before the onset of the dry period, owing to the adaptation by the vegetation to avoid severe drought stress. Although it is unclear how the ecosystem's photosynthesis might respond to the drier environment in the future, lack of such adaptation might cause disruption in the photosynthetic component of the CO_2 exchange, thus could alter the ecosystem's CO_2 dynamic.

The secondary peat swamp forest had functioned as a net CO_2 sink of 136 ± 51 g C m^{-2} year-1 during the four years (**Table 5**). In comparison with flux studies using the eddy

covariance technique in tropical humid forest, the negative annual NEE was equivalent to those of tropical rain forests on mineral soil in Peninsula Malaysia (-124 g C m^{-2} year-1, Kosugi et al., 2008) and in French Guiana (-138 g C m^{-2} year-1, Bonal et al., 2008), whereas it was less negative than the mean of 29 tropical humid evergreen forests (-403 ± 102 g C m^{-2} year-1 (originally in NEP), Luyssaert et al., 2007). In contrast, the annual NEE (-136 g C m^{-2} year-1) was more negative than that of an almost undrained PSF in Central Kalimantan, Indonesia (Hirano et al., 2012); mean annual NEE was 174 ± 203 g C m^{-2} year-1 for four years including an El Niño event. The large NEE difference of 310 g C m^{-2} year-1 on average between the two sites (Hirano et al. – this study) resulted from both GPP (-214 g C m^{-2} year-1) and RE (96 g C m^{-2} year-1) differences. The higher GPP in this study was attributable to higher PAI; 7.9 m^2 m^{-2} (this study) vs. 5.0 m^2 m^{-2} (Hirano et al., 2012). The lower RE in this study was probably due to higher minimum GWL despite similar mean annual GWL (-19 cm vs. -14 cm); GWL lowered to -1 m on a monthly basis in 2006, an El Niño year, even at the almost undrained PSF in Central Kalimantan. The annual NEE showed a negative linear relationship with annual mean GWL (r^2 = 0.92), though it was not significant (p = 0.08) because of a small sample size (n = 4). If the significance level of $p < 0.10$ is allowed, the linearity suggests that every lowering of GWL by 10 cm increases NEE by 133 g C m^{-2} year-1. Such linearity between annual NEE and annual mean GWL was also found in PSFs in Central Kalimantan with the slopes of 238 and 161 g C m^{-2} year-1 against 10-cm GWL lowering, respectively, in the almost undrained and drained PSFs (Hirano *et al.*, 2012). In this site, the sensitivity of NEE to GWL was probably lower than those in Central Kalimantan (CK). The difference might be related to differences in peat depth (10 m (this study) vs. 3-4 m (CK)) and peat formation history (costal peat (this study) vs. inland peat (CK), Dommain et. al. (2011)).

To assess C balance, not only eddy CO_2 flux but also C leaching through water discharge should be considered. Moore et al. (2013) reported that 62.5 and 105.3 g C m^{-2} year-1 were lost as organic carbon (dissolved organic carbon (DOC) + particulate organic carbon (POC)), respectively, from an intact peat swamp forest and a moderately disturbed peat swamp forest in Central Kalimantan. Moreover, about 10 g C m^{-2} year-1 of annual methane emissions was assessed in a nearby undrained tropical peat swamp forest in Sarawak (Wong *et al.*, 2018). Thus, if these C losses are considered, the secondary peat swamp forest could be a slight C sink or a C neutral.

3.3. Conclusions

This study showed the CO_2 balance of a secondary peat swamp forest developed in a humid climate with a relatively short dry period. RE was the main controller of the seasonal variation in NEE and was negatively related to GWL. This result showed that the response of RE to GWL in the forest was similar to previous studies. El Niño was predicted to increase in intensity in the western area of the equatorial Pacific Ocean (Power *et al.*, 2013). The frequency of drought also predicted to increase in the eastern area of Indian Ocean, as Cai et al. (2014) forecasts that extremely strong positive Indian Ocean Dipole (IOD) modes will increase in the future. Such changes in climate may potentially shift the almost C neutral PSF to a C source in the future under the drier environment.

Chapter 4: CARBON DIOXIDE BALANCE OF AN OIL PALM PLANTATION

4.1.Results

4.1.1. Microclimates and GWL conditions

Annual PTs in the OPP was considerably large, exceeding 2800 mm from 2011 to 2014. Although La Niña occurred from 2010 to early 2012, large increase in annual PT only observed in 2012 (**Table 6**). Low monthly PT (< 100 mm month^{-1}) was only observed in July 2011, September 2013, February 2014, and June to July 2014 (**Figure 11**a). Despite the occurrence of 3 dry months in 2014, PT in January and December rose above 500 mm, causing no decrease in annual PT. Even though the seasonal variation of PT was not clear in this region, period between July to September were relatively dry. In 2011, lower PT from July to September caused GWL to drop and reach the minimum of -105 cm at the end of September (**Figure 11**b). Daily mean GWL fluctuated between -125 to -17 cm throughout the study period. From 2012 to 2013 daily GWL were maintained above -84 cm. However, VWC in 2013 showed a decreasing pattern toward June before it gradually increased toward the end of the year (**Figure 11**c). Significant drop in GWL in February 2014 also caused significant decrease in VWC. Unfortunately, VWC data were lost after the March 2014. In addition, during the two dry periods in 2014 GWL also dropped below -100 cm.

Daily PPFD varied between 6 to 51 mol m^{-2} day^{-1} (**Figure 11**d) with annual sums between 12.3 to 12.7 kmol m^{-2} year^{-1} (**Table 6**). Seasonal variation of PPFD was weak, however, relatively low PPFD were observed between December and January every year. The large PT during those periods most likely increased the frequency of cloud cover during rain event which blocked incoming solar radiation. Daily mean T_a was also generally lower during the high PT period but increased to reach its peak at the beginning of June before it gradually decreased following the onset of the wet period (**Figure 11**e). Seasonal variation of

midday VPD was generally similar to T_a (**Figure 11**f). However, in 2011, midday VPD dropped during the peak of T_a in early June.

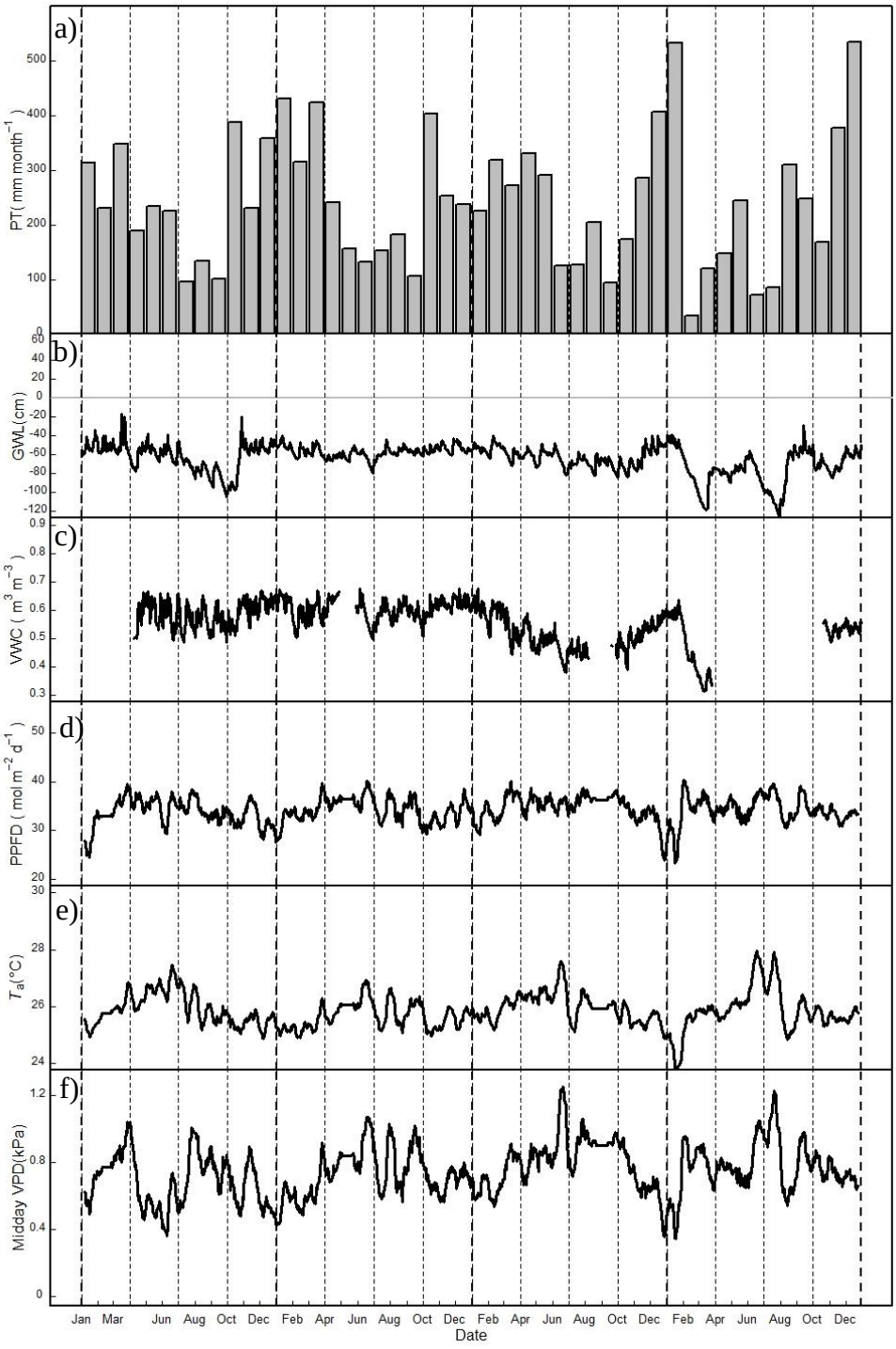

Figure 11. *Environmental condition in OPP: monthly precipitation (PT) (a), daily mean groundwater level (GWL) (b), daily mean of volumetric water content (VWC) (c), daily photosynthetic photon flux density (PPFD) (d), daily mean air temperature (T_a) (e) and daytime mean vapor pressure deficit (VPD) (f) from January 2011 to December 2014. Black lines are 14-day-long moving averages. Bold dashed vertical lines are the border of calendar years.*

4.1.2. Controlling factors of CO_2 fluxes

PPFD was the main controlling factor of NEE during the daytime. During the daytime, NEE showed a typical curvilinear relationship with PPFD because of photosynthesis by plants (**Figure 12**). In **Figure 12** half-hourly daytime NEE was fitted with (Equation *6*) to obtain the photosynthetic parameters (P_{max}. α, and RE_d) of the ecosystem. The light response curve also fitted on daily basis to assess the seasonal variation of the photosynthetic parameters. The relationship showed that NEE sharply decreased (more negative) in the morning as PPFD started to increase. The initial slope (PPFD < 500 µmol m^{-2} s^{-1}) of the relationship which represent the apparent quantum yield (α) was estimated at 0.04±0.03 mol CO_2 mol $photon^{-1}$. The slope of the light response curve gradually decreased as PPFD approaching the value of 1200 µmol m^{-2} s^{-1}. Therefore, this will be used as the saturation point of the relationship.

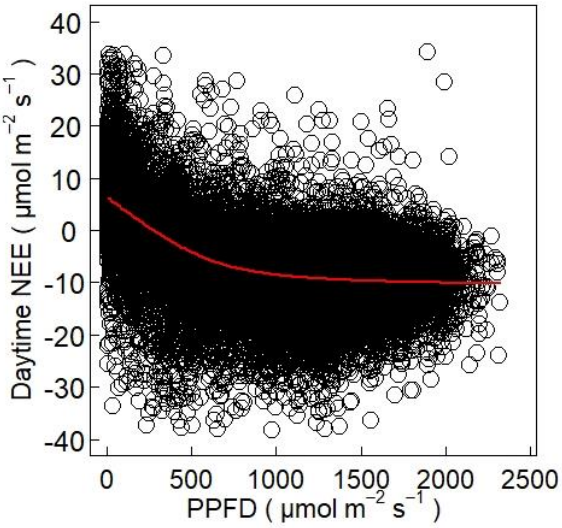

Figure 12. Daytime NEE response to PPFD. A non-rectangular hyperbola function was fitted to half-hourly data (red line).

Then, the response of daytime NEE to air dryness (VPD) can be analysed using the relationship between light saturated NEE (PPFD > 1200 µmol m^{-2} s^{-1}) and VPD (**Figure 13**). This analysis is important to analyse the response of stomata opening to air dryness. Light saturated NEE exhibited a significant positive linear relationship with VPD (P < 0.001). The relationship suggested NEE increased by 0.55 µmol m^{-2} s^{-1} with 0.1 kPa increase in VPD.

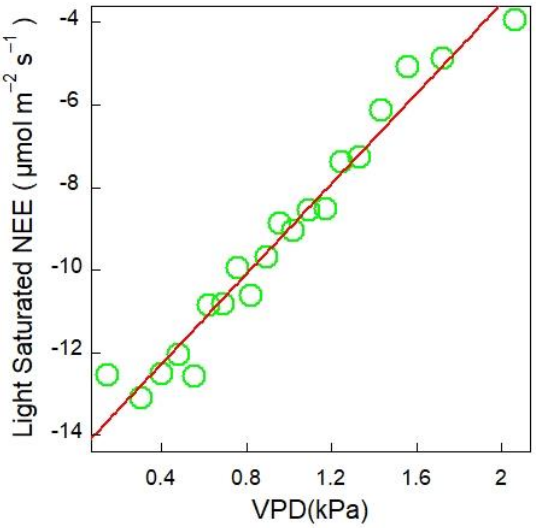

Figure 13. *Relationship between light saturated NEE (PPFD > 1200 µmol m^{-2} s^{-1}) and VPD. Significant line (P < 0.001) are drawn in red.*

The response of RE to environmental factors was assessed using half-hourly nighttime NEE. In OPP, RE only showed significant relationship with GWL and VWC (P <0.05, **Figure 14**), where RE increased as GWL (R^2=0.22, P <0.05) or VWC (R^2=0.21, P <0.05) increased. RE increased by 0.32 µmol m^{-2} s^{-1} for every 10 cm increase in GWL (**Figure 14**a). The intercept of the relationship was 11.5 µmol m^{-2} s^{-1}. Furthermore, every 0.1 m^3 m^{-3} increased in VWC, RE increased by 0.62 µmol m^{-2} s^{-1} (**Figure 14**b). However, the strength of both relationships were indistinguishable. Even though the relationships were significant, the R^2 is low (0.22 and 0.21 respectively for GWL and VWC).

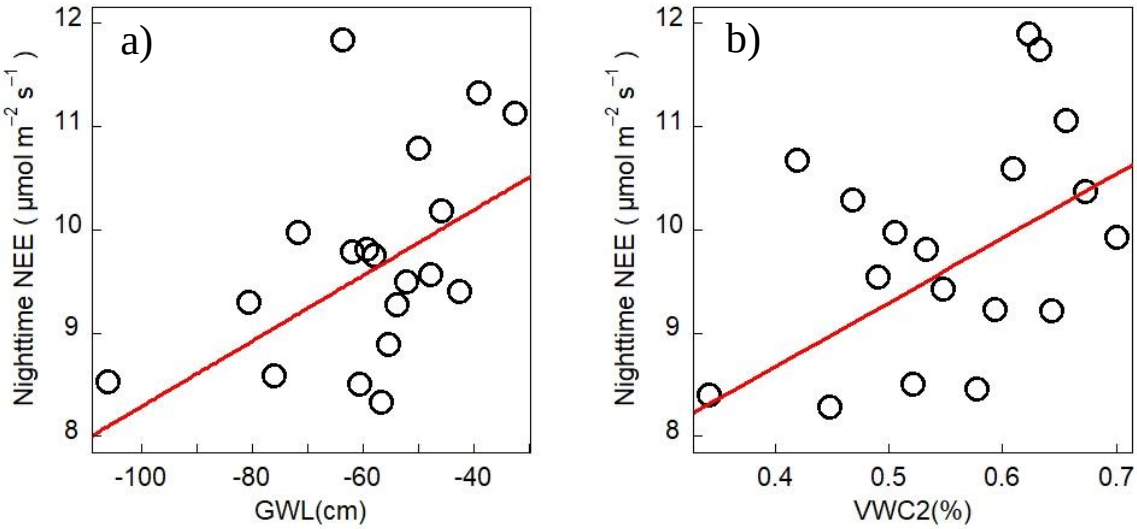

Figure 14. *Relationship between nighttime NEE and GWL (a) or VWC (b). Red lines are drawn for significant correlation (P < 0.05).*

4.1.3. Seasonality of CO_2 fluxes

Figure 15 shows the seasonal variation of daily NEE, RE, and GPP. Daily NEE was averaged at 2.7±2.8 g C m^{-2} day^{-1} from 2011 to 2014. Daily RE and GPP were 9.7±2.6 and 7.0±1.5 g C m^{-2} day^{-1}, respectively, throughout the study period. No clear seasonality was found in daily NEE, RE, and GPP. However, variations in daily RE explained 70% of the variation in daily NEE (r2 = 0.70). Simple linear regression analysis suggested daily NEE increased by 0.9 g C m^{-2} day^{-1} with 1.0 g C m^{-2} day^{-1} increase in daily RE ($P < 0.001$). On the other hand, variation in daily GPP only explained 15% of the variation in daily NEE (r2 = 0.15).

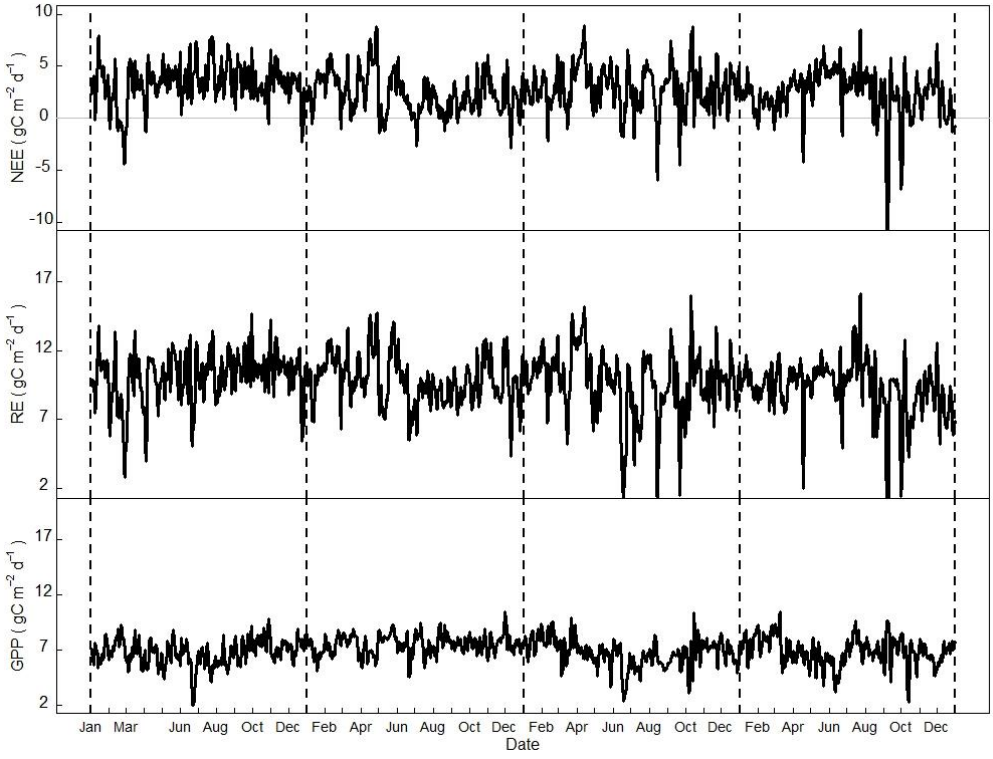

Figure 15. *Seasonal variation of daily NEE, RE, and GPP from 2011 to 2014.*

Figure 16 showed the seasonal variation of daily P_{max}, α, and RE_d. P_{max} fluctuated between 8.17 and 57.69 µmol m^{-2} s^{-1} from 2011 to 2014. α was ranged between 0.00 to 0.11 mol CO_2 mol $photon^{-1}$. On the other hand, RE_d took the value between 0.25 to 20.00 µmol m^{-2} s^{-1}. All the photosynthetic parameters did not show any significant seasonal variation.

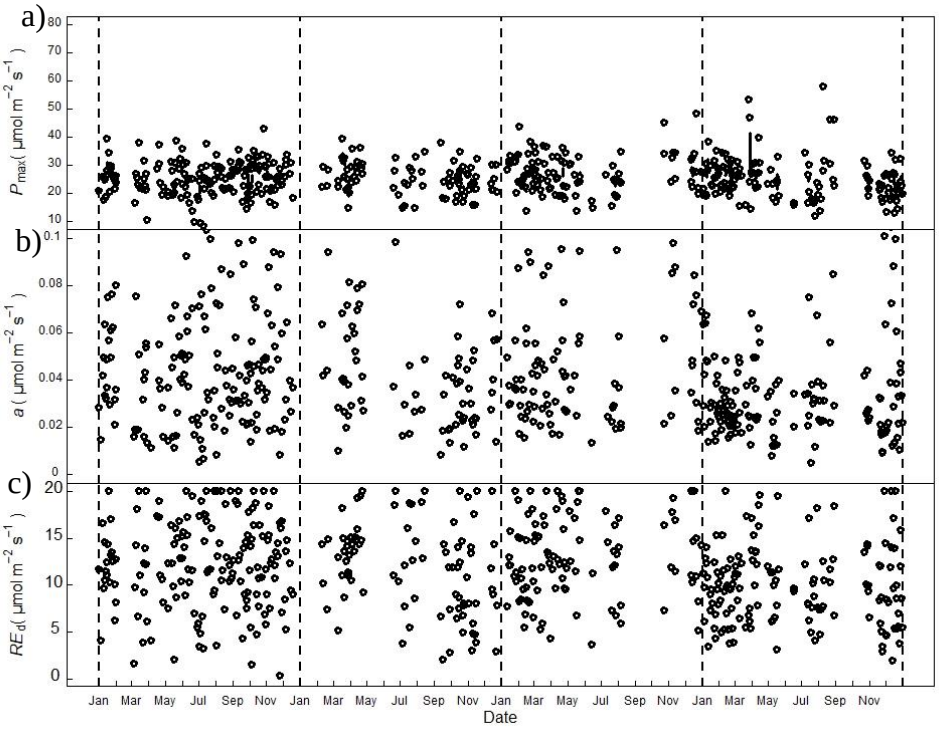

Figure 16. *Seasonal variation of P_{max} (a), α (b), and RE_d (c) obtained from light-response curve fitting. A non-rectangular hyperbola function was fitted to half hourly daytime NEEs.*

4.1.4. Aboveground Biomass

Using allometric equation developed by Khasanah et al. (2015), AGB of the OPP was estimated from the tree height measurements. AGB was estimated at 1071 gC m^{-2} in March 2011 and increased to 2845 gC m^{-2} in January 2015. This account for AGB increment of 1463 gC m^{-2} year^{-1}.

4.1.5. Annual CO_2 budget

OPP was a net CO_2 source within the study period with annual NEE ranging between 849 to 1223 gC m^{-2} year^{-1}, in 2014 and 2011 respectively (**Table 6**). The positive NEE of 995±181 gC m^{-2} year^{-1} was the result from large annual RE of 3546±141 gC m^{-2} year^{-1} compared to lower annual GPP of 2552±135 gC m^{-2} year^{-1}. Annual RE increased by 150 gC m^{-2} year^{-1} when annual mean GWL increased by 10 cm, though the relationship was not

significant (P=0.186, R^2=0.66), probably due to limited number of data. Annual GPP showed significant positive relationship with annual sum of PT (P=0.003, R^2=0.99), whereas no significant relationship was found with annual PPFD.

Year	NEE	RE	GPP	PPFD	PT	GWL
	gC m^{-2} $year^{-1}$			kmol m^{-2} $year^{-1}$	mm	cm
2011	1223	3822	2476	12.3	2850	-61.9
2012	851	3582	2750	12.6	3034	-57.0
2013	1058	3803	2461	12.7	2854	-62.6
2014	849	3445	2517	12.5	2873	-74.8
Mean±SD	995±181	3663±182	2552±135	12.5±0.2	2903±88	-64.1±7.6

Table 6. *Annual CO_2 balance and annual mean of environmental variables from 2011 to 2014 on a calendar basis in OPP.*

4.2. Discussion

The climate in the study site was considered as wet all year round, because the monthly PT seldom lowered less than 100 mm (**Figure 11**). In addition, the GWL in the study site was controlled resulting in no significant variation in hydrological condition. Daily GWL was generally maintained above -80 cm from 2011 to 2013 but dropped below -120 cm during the driest months in 2014. However, no significant increase in RE was observed during the abnormally dry months. The relationship between the nighttime NEE and GWL and VWC also suggested RE decreased with the decreasing GWL or VWC. On the contrary, Ishikura et al. (2018) using an automated chamber system found that RS was negatively correlated with GWL and water-filled pore space (WFPS). The discrepancy might suggest that the variation in RE are not dominated by RS but rather come from other emission sources.

The OPP was a net CO_2 source from 2011 to 2014 (995±181 gC m^{-2} $year^{-1}$, **Table 6**). This was about 3.5 times larger than the mean of 29 tropical humid evergreen forests (−403 ± 102 gC m^{-2} $year^{-1}$, Luyssaert et al., 2007). The large source is mainly caused by the low annual GPPs compared to PSF (31% lower), and comparable annual RE (**Table 5** vs **Table 6**). The estimated annual GPP of 2552±135 gC m^{-2} $year^{-1}$ was slightly lower than those reported by Tan, Devi, Bin, & Philip, (2011) (2924±30 gC m^{-2} $year^{-1}$), but 28% lower than that of tropical humid evergreen forest reported by Luyssaert *et al.* (2007). Because RE was similar to that of PSF, increased emission from other sources are the more likely explanation. In peatlands, enhanced emission is common following GWL lowering. エラー! 参照元が見つかりません。 showed the annual soil respiration (RS) from primary peat swam forest (PPSF), PSF, and OPP using the manual and automated chamber method. Melling (2013) measured RS using manual chamber at PSF and OPP used in this study and in a PPSF from January to December 2011. Automated soil chamber data used here was obtained from the same site from 2015 to 2016 (Ishikura et al., 2018; Ishikura et al., unpublished).

Unfortunately, automated chamber data from PSF were excluded due to poor quality. Both manual chamber and automated chamber methods showed lower RS in OPP compared to PPSF. The order of RS from the highest to lowest are PPSF > PSF > OPP (Melling, 2013). Annual RS from the automated chamber system seems to agree with the manual chamber method. The lower RS in OPP despite the lower GWL compared to PPSF and PSF might be due to the low soil gas diffusiveness. As reported by Adachi et. al. (2006) high bulk density increased WFPS which lead to low gas diffusiveness. With the expected low plant respiration and low RS, emission from other source(s) could be dominant in OPP.

In OPP, large amount of tree stumps and debris left over from land clearing remains on the soil. In addition, leaf litter of oil palm trees also accumulated and stacked in a "stacking row" during harvesting. All these sources have never been quantified so far. The positive relationship between RE and GWL and VWC might be associated with drying and wetting of plants remnants (including litterfall) on the soil rather than direct effect of GWL. Similar suppression of RE during the dry season was reported by Goulden et al. (2004) in an old-growth Amazonian forest. In addition, Wieder et. al. (2009) showed that mass loss rates of litter increased with increasing PT.

4.3. Conclusion

This study presented the CO_2 balance of an oil palm plantation developed on peat with controlled GWL. The OPP act as a net CO_2 source during the 4-year period from 2011 to 2014. Variation in NEE was mainly associated with the variation in RE. The response of the CO_2 balance in OPP to GWL was unclear due to low fluctuation in GWL caused by plantation water management. Narrow fluctuation of GWL induced by plantation water management could be the reason.

Chapter 5: EFFECT OF LAND CONVERSION ON ECOSYSTEM-SCALE CARBON DIOXIDE BALANCE

5.1. Impact on microclimate

One of the most noteworthy changes after forest conversion to OPP is the changes in vegetation cover. The dense canopy forest is replaced by much sparser crop. In forest, dense canopy provides shading to the vegetation under the canopy, as well as the top soils. Such structure largely influenced into the microclimate within the canopy. Denser canopy allows less solar radiation to penetrate the canopy. Other than that, the movement of air within the canopy also can be dependent on the canopy structure. Thus, changes in vegetation cover can cause significant changes in local climates. By altering the local climate, land use change can influence both biodiversity and ecological processes. Luskin and Potts (2011) reported a 2.8 °C temperature increase in an oil palm plantation from forest in Southeast Asia region, which was also accompanied by substantial reduction in humidity.

Figure 17 shows the mean diurnal variation of T_a measured above and below the canopy at each site. At the forest site minimum above canopy T_a of 23.9 °C was observed at 07:00 and reached maximum of 30.5 °C at 15:00. On the other hand, minimum above canopy T_a was observed half hour earlier at 06:30, taking the value of 23.0 °C. Maximum T_a of 30.3 °C at OPP was similar to that of PSF, but occurred half hour prior at 14:30. Under canopy, minimum T_a at PSF and OPP were both observed at 06:30, with respective values of 23.6 °C and 23.0 °C. Maximum below canopy T_a at the OPP was 1.0 °C higher than the peak value of 30.3 °C at the PSF.

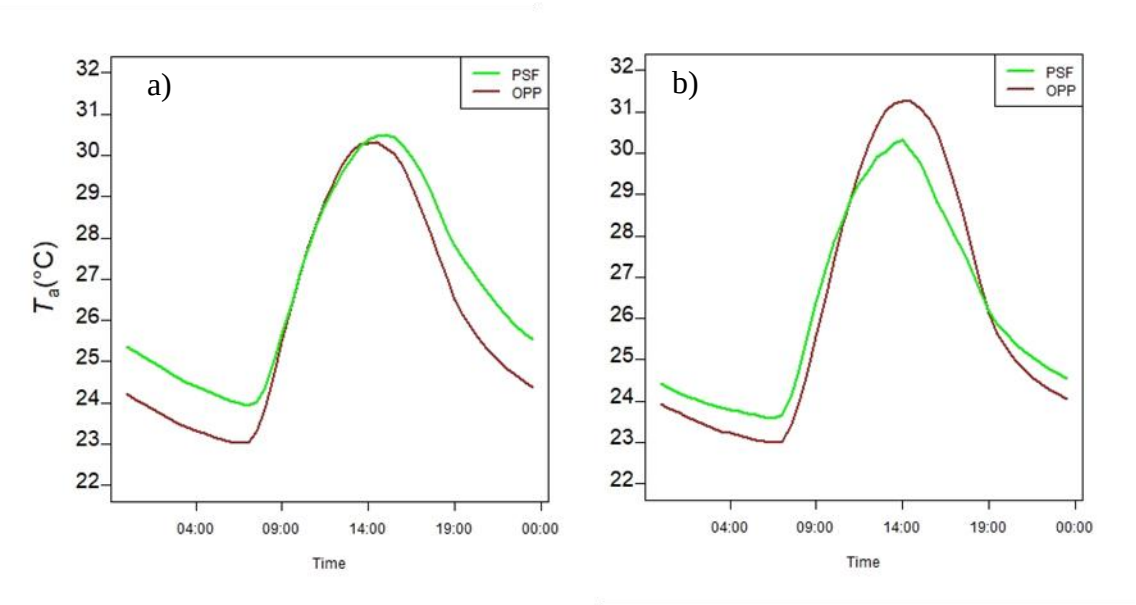

Figure 17*. Mean diurnal variation of air temperature measured a) above canopy and b) below canopy from May to December 2014. Air temperature above canopy were measured at 41 m and 21 m respectively in PSF and OPP. The below canopy temperature sensors were installed at 3 m height at both sites.*

The higher below canopy T_a at OPP was attributable to the low PAI at the study site due to sparser vegetation cover. Vegetation cover influenced the local climate through three main mechanisms (Hardwick *et al.*, 2015). The first is through absorption, scattering and reflection of solar radiation. This reduced significant amount of energy entering the below canopy air including the soil. The amount of blocked solar radiation relies heavily on the ecosystem PAI. The second mechanism is associated with the turbulent mixing within the canopy, where dense canopies allow less turbulent mixing than sparse canopies. Turbulent mixing can force hot air from the heated top layer of the canopy downward during the day. The last mechanism is associated with how the T_a affect the relative humidity in the ecosystem. Higher T_a tend to reduce relative humidity.

Soil heating from direct penetration of solar radiation and heat transfer from near ground T_a are likely to increase near surface soil temperature on peat. Hirano *et al.* (2009) showed that the dependency of CO_2 emission to temperature in the tropic are similar to other

forest ecosystems in higher latitude. Therefore, any temperature increase in tropical peatlands ecosystem could make the ecosystem become more vulnerable to disturbance.

5.2. Changes in carbon dioxide balance

In this study, the OPP was a net CO_2 source (995±181 gC m^{-2} $year^{-1}$) and the PSF was a moderate CO_2 sink (-136±51 gC m^{-2} $year^{-1}$). The large source was mainly due to the lower GPP in OPP compared to PSF (2552±135 vs. 3682 ± 149 gC m^{-2} $year^{-1}$). Given the low GPP, RE in OPP also regarded as considerably large, as it matched those in PSF with much larger GPP (3663 ± 182 vs. 3546 ± 149 g C m^{-2} $year^{-1}$ respectively for OPP and PSF). These values were 16 to 20% larger than the mean of tropical humid evergreen forests reported by Luyssaert et al. (2007) (3061 ± 162 g C m^{-2} $year^{-1}$). In similar ecosystem but drier environment in Central Kalimantan, Hirano et al. (2012) reported similar large annual RE (3642 ± 115 and 3519 ± 132 g C m^{-2} $year^{-1}$). Annual GPP of 3682 ± 149 g C m^{-2} $year^{-1}$ in PSF was slightly larger than that of tropical humid evergreen forests (3551±160 g C m^{-2} $year^{-1}$) and undrained PSF in Kalimantan (3468 ± 118 g C m^{-2} $year^{-1}$). Dense canopy as indicated by high LAI of 8.20 m^2m^{-2} might be a good explanation for the large GPP. In addition, PSF used in this study are a regenerated forest with rapidly growing trees. RE in most PSF are generally larger than other types of tropical forest. Therefore, its net sink of CO_2 is highly dependent on the magnitude of GPP, induced by the vegetation cover.

Site	P_{max}	α	RE_d
	μmol m^{-2} s^{-1}	mol CO_2 mol $photon^{-1}$	μmol m^{-2} s^{-1}
PSF	41.7±21.0 [a]	0.04±0.02 [a]	9.9±5.1 [a]
OPP	27.9±15.9 [b]	0.05±0.03 [a]	11.4±4.8 [b]

Table 7. *Unpaired t-test results for light response curve photosynthetic parameters. Mean±SD marked with different letter are significantly different.*

Direct field measurement from study showed that large reduction in GPP occurred following PSF conversion to OPP. Even though annual GPP was lower in OPP, the AGB increment was 57.4% larger than that of PSF (459 vs. 292 g C m^{-2} $year^{-1}$), indicating rapid growth of the oil palm trees as compared to forests. On the other hand, only slight increase in RE was observed after conversion. Enhanced peat oxidation is normally expected following peatlands conversion due to GWL lowering (Furukawa *et al.*, 2005; Couwenberg, 2011). However, this study illustrates no significant increase in RE after conversion. In fact, RS from manual and automated chamber showed lower RS in OPP compared to forest (**Figure 18** エラー! 参照元が見つかりません。). The low RS despite lower GWL could be associated with the low gas diffusiveness due to high bulk density. High bulk density resulted in compaction and the consolidation of the soil. Moreover, the positive correlation between RE and GWL in this study also could be a good indicator of unalignment between RS and RE.

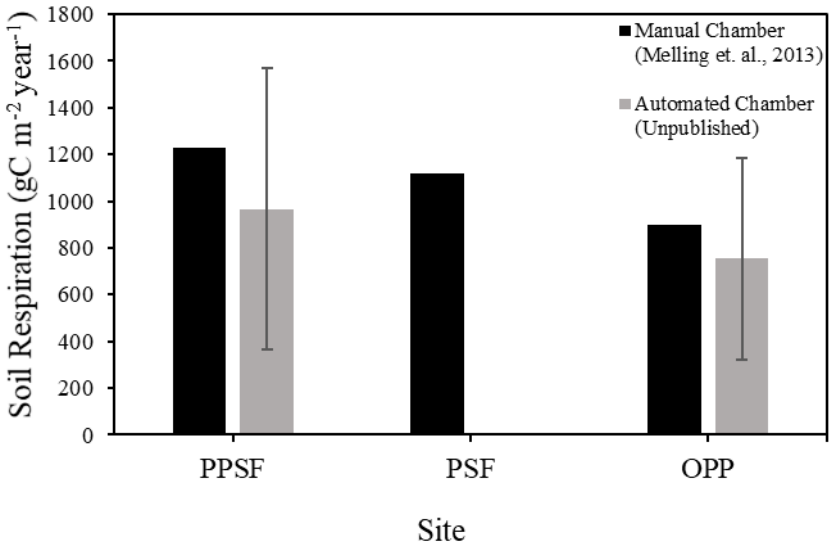

Figure 18. *Annual soil respiration from primary peat swamp forest (PPSF), PSF, and OPP obtained from manual and automated chamber method.*

Figure 19 エラー! 参照元が見つかりません。 illustrate the CO_2 pathways between PSF and OPP. CO_2 emitted through litter and debris was estimated to contribute

about 41% of total RE in OPP. Therefore, this could be the main emission source after PSF converted into OPP. However, there is still no published study conducted in OPP on peat that considering such respiration components. Most current studies in OPP on peat focussed on the changes in RS following GWL lowering.

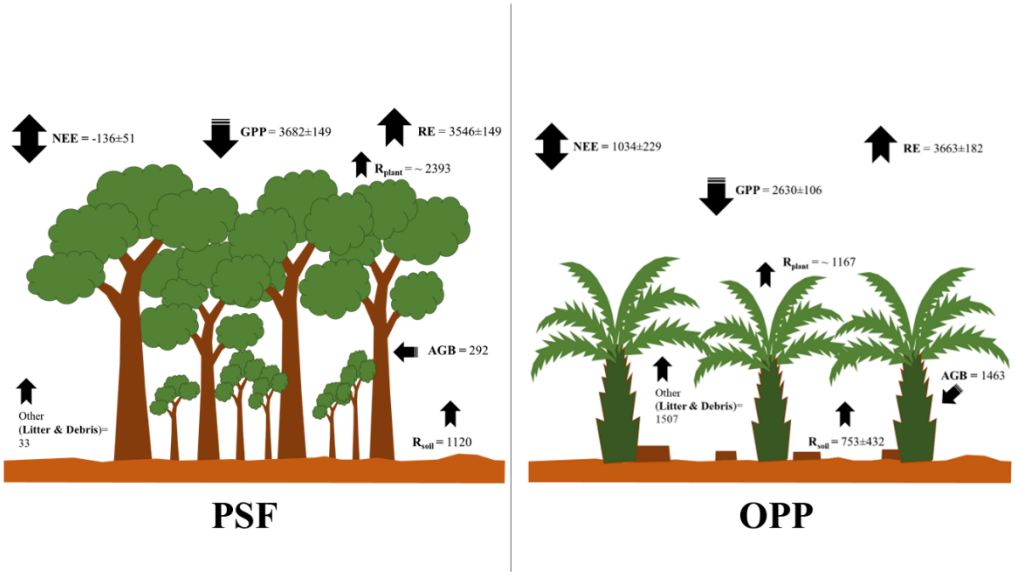

Figure 19. *CO_2 pathway before and after conversion. Values are presented in g C m^{-2} $year^{-1}$.*

Although it this study did not determine C loss from other process such as dissolve organic C (DOC), particulate organic C (POC) and dissolved inorganic C (DIC), the soil C content in both site showed similar decreasing trend (**Figure 20**). In PSF soil C content at 0-25 cm decreased to 51.2% in 2014 from 52.9% in 2011. Soil C content in OPP was 56.0% in 2011 and 54.3% in 2014. In 4 years period both ecosystem loss 1.7% of its C content. Relatively higher C content in OPP was mainly due to the distinct forest type, where the OPP was a former mixed peat swamp forest while PSF site was located in near the center of the peat dome.

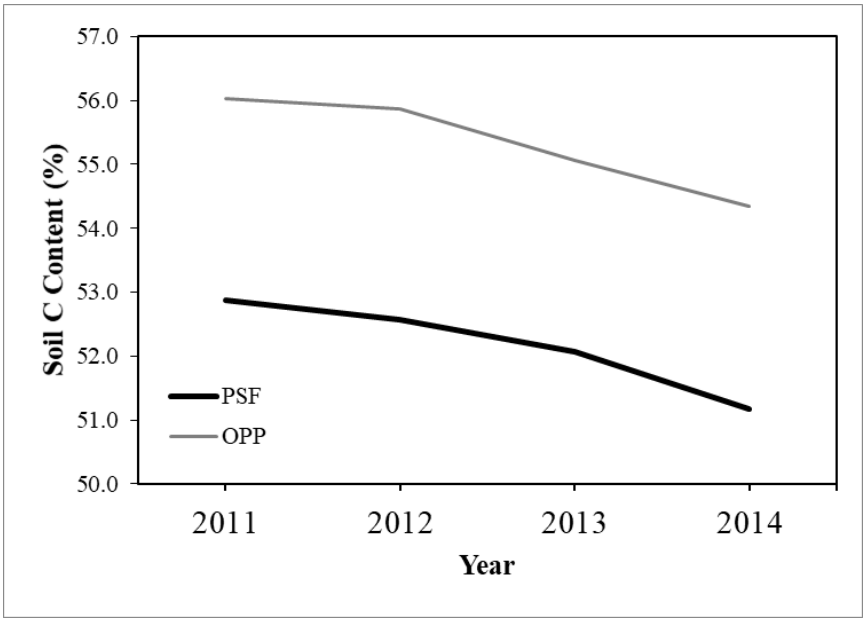

Figure 20. *Total soil C content of PSF and OPP from 2011 to 2014*

Chapter 6: GENERAL CONCLUSION

NEE was measured during a 4 years period from 2011 to 2014 in an OPP and a PSF. Each ecosystem was used to represent the condition before and after land conversion. The PSF was a modest CO_2 sink, whereas OPP was a large CO_2 source. Seasonal variation of RE greatly influenced the variation of NEE in the PSF. RE was sensitive to GWL similar to the previous studies. Similarly, in OPP, variation in NEE was mainly governed by variation in RE. However, inverse relationship was found between RE and GWL.

The large source following conversion was partly due to the low GPP in OPP. However, the respiration components were a little complicated. Soil chamber measurement indicates reduced RS despite the lower GWL after conversion. This suggests that CO_2 emitted from leaf litter and plant debris might be the dominant source after conversion. Removing huge tree stumps and debris before planting can be a good strategy to reduce emissions. This could be a valuable insight for reducing CO_2 emission in OPP on peat.

However, further studies that include all respiration components in OPP are necessary to support such a hypothesis.

References

Adachi M, Bekku YS, Rashidah W, Okuda T and Koizumi H 2006: Differences in soil respiration between different tropical ecosystems. Applied Soil Ecology. doi: 10.1016/j.apsoil.2006.01.006.

Anderson JAR 1964: The structure and development of the peat swamps of Sarawak and Brunei. The Journal of Tropical Geography, 18, pp. 7–16.

Bonal D, Bosc A, Ponton S, *et al.* 2008: Impact of severe dry season on net ecosystem exchange in the Neotropical rainforest of French Guiana. Global Change Biology, 14(8), pp. 1917–1933. doi: 10.1111/j.1365-2486.2008.01610.x.

Cai W, Santoso A, Wang G, Weller E, Wu L, Ashok K, Masumoto Y and Yamagata T 2014: Increased frequency of extreme Indian Ocean Dipole events due to greenhouse warming. Nature, 510(7504), pp. 254–258. doi: 10.1038/nature13327.

Corley and Tinker 2003: The Classification and Morphology of the Oil Palm. The Oil Palm. doi: 10.1002/9780470750971.ch2.

Couwenberg J 2011: Greenhouse Gas Emissions from Managed Peat Soils : Is The IPCC Reporting Guidance Realistic ? Mires and Peat,. doi: citeulike-article-id:13916340.

Dargie GC, Lewis SL, Lawson IT, Mitchard ETA, Page SE, Bocko YE and Ifo SA 2017: Age, extent and carbon storage of the central Congo Basin peatland complex. NatureNature Publishing Group, 542(7639), pp. 86–90. doi: 10.1038/nature21048.

Dommain R, Couwenberg J and Joosten H 2011: Development and carbon sequestration of tropical peat domes in south-east Asia: Links to post-glacial sea-level changes and Holocene climate variability. Quaternary Science Reviews, 30(7–8), pp. 999–1010. doi: 10.1016/j.quascirev.2011.01.018.

France PC, Willem J, Friedlingstein P and Munhoven G 2013: Carbon and Other Biogeochemical Cycles 6. 5th Assessment IPCC, Chapter 6(June), p. 2012. doi: 10.1017/CBO9781107415324.015.

Furukawa Y, Inubushi K, Ali M, Itang AM and Tsuruta H 2005: Effect of changing groundwater levels caused by land-use changes on greenhouse gas fluxes from tropical peat lands. Nutrient Cycling in Agroecosystems, 71(1), pp. 81–91. doi: 10.1007/s10705-004-5286-5.

Goulden ML, Miller SD, Da Rocha HR, Menton MC, De Freitas HC, E Silva Figueira AM and Dias De Sousa CA 2004: Diel and seasonal patterns of tropical forest CO2 exchange. Ecological Applications, 14(4 SUPPL.), pp. 42–54. doi: 10.1890/02-6008.

Grace J, Lloyd J, McIntyre J, Miranda A, Meir P, Miranda H, Moncrieff J, Massheder J, Wright I and Gash J 1995: Fluxes of carbon dioxide and water vapour over an undisturbed tropical forest in south-west amazonia. Global Change Biology. doi: 10.1111/j.1365-2486.1995.tb00001.x.

Hardwick SR, Toumi R, Pfeifer M, Turner EC, Nilus R and Ewers RM 2015: The relationship between leaf area index and microclimate in tropical forest and oil palm plantation: Forest disturbance drives changes in microclimate. Agricultural and Forest Meteorology. doi: 10.1016/j.agrformet.2014.11.010.

Hartmann DJ, Klein Tank AMG, Rusticucci M, *et al.* 2013: Observations: Atmosphere and Surface. Climate Change 2013: The Physical Science Basis. Contribution of Working Group I to the Fifth Assessment Report of the Intergovernmental Panel on Climate Change, pp. 159–254. doi: 10.1017/CBO9781107415324.008.

Hirano T, Jauhiainen J, Inoue T and Takahashi H 2009: Controls on the carbon balance of tropical peatlands. Ecosystems, 12(6), pp. 873–887. doi: 10.1007/s10021-008-9209-1.

Hirano T, Kusin K, Limin S and Osaki M 2014: Carbon dioxide emissions through oxidative peat decomposition on a burnt tropical peatland. Global Change Biology, 20(2), pp. 555–565. doi: 10.1111/gcb.12296.

Hirano T, Segah H, Harada T, Limin S, June T, Hirata R and Osaki M 2007: Carbon dioxide balance of a tropical peat swamp forest in Kalimantan, Indonesia. Global Change Biology, 13(2), pp. 412–425. doi: 10.1111/j.1365-2486.2006.01301.x.

Hirano T, Segah H, Kusin K, Limin S, Takahashi H and Osaki M 2012: Effects of disturbances on the carbon balance of tropical peat swamp forests. Global Change Biology, 18(11), pp. 3410–3422. doi: 10.1111/j.1365-2486.2012.02793.x.

Hooijer A, Page S, Jauhiainen J, Lee WA, Lu XX, Idris A and Anshari G 2012: Subsidence and carbon loss in drained tropical peatlands. Biogeosciences, 9(3), pp. 1053–1071. doi: 10.5194/bg-9-1053-2012.

van Huissteden J, van den Bos R and Marticorena Alvarez I 2006: Modelling the effect of water-table management on CO2 and CH4 fluxes from peat soils. Geologie en Mijnbouw/Netherlands Journal of Geosciences. doi: 10.1029/2005JG000010; Vermeulen, J., Hendriks, R.F.A., Bepaling van afbraaksnelheden van organische stof in laagveen (1996), Ademhalingsmetingen aan ongestoorde veenmonsters in het laboratorium. Rapport 288, DLO-Staring Centrum (Wageningen)Verville, J.H., Hobbie, S.E., Chapin III, F.S., Hooper, D.U., Response of tundra CH4 and CO2 flux to manipulation of temperature and vegetation (1998) Biogeochemistry, 41, pp. 215-235; Walter, B.P., A process-based, climate-sensitive model to derive methane em.

Ishikura K, Hirano T, Okimoto Y, *et al.* 2018: Soil carbon dioxide emissions due to oxidative peat decomposition in an oil palm plantation on tropical peat. Agriculture, Ecosystems and EnvironmentElsevier, 254(September 2017), pp. 202–212. doi: 10.1016/j.agee.2017.11.025.

Jauhiainen J, Hooijer A and Page SE 2012: Carbon dioxide emissions from an Acacia plantation on peatland in Sumatra, Indonesia. Biogeosciences, 9(2), pp. 617–630. doi: 10.5194/bg-9-617-2012.

Jauhiainen J, Page SE and Vasander H 2016: Greenhouse gas dynamics in degraded and restored tropical peatlands. Mires and Peat, 17, pp. 1–12. doi: 10.19189/MaP.2016.OMB.229.

Jauhiainen J, Silvennoinen H, Könönen M, Limin S and Vasander H 2016: Management driven changes in carbon mineralization dynamics of tropical peat. Biogeochemistry, 129(1–

2), pp. 115–132. doi: 10.1007/s10533-016-0222-8.

Khasanah N, van Noordwijk M and Ningsih H 2015: Aboveground carbon stocks in oil palm plantations and the threshold for carbon-neutral vegetation conversion on mineral soils. Cogent Environmental ScienceCogent, 1(1), pp. 1–18. doi: 10.1080/23311843.2015.1119964.

Koh LP, Miettinen J, Liew SC and Ghazoul J 2011: Remotely sensed evidence of tropical peatland conversion to oil palm. Proceedings of the National Academy of Sciences of the United States of America, 108(12), pp. 5127–32. doi: 10.1073/pnas.1018776108.

Konecny K, Ballhorn U, Navratil P, Jubanski J, Page SE, Tansey K, Hooijer A, Vernimmen R and Siegert F 2016: Variable carbon losses from recurrent fires in drained tropical peatlands. Global Change Biology, 22(4), pp. 1469–1480. doi: 10.1111/gcb.13186.

Könönen M, Jauhiainen J, Laiho R, Spetz P, Kusin K, Limin S and Vasander H 2016: Land use increases the recalcitrance of tropical peat. Wetlands Ecology and Management, 24(6), pp. 717–731. doi: 10.1007/s11273-016-9498-7.

Kosugi Y, Takanashi S, Ohkubo S, Matsuo N, Tani M, Mitani T, Tsutsumi D and Nik AR 2008: CO2 exchange of a tropical rainforest at Pasoh in Peninsular Malaysia. Agricultural and Forest Meteorology, 148(3), pp. 439–452. doi: 10.1016/j.agrformet.2007.10.007.

Lampela M, Jauhiainen J, Kämäri I, Koskinen M, Tanhuanpää T, Valkeapää A and Vasander H 2016: Ground surface microtopography and vegetation patterns in a tropical peat swamp forest. CatenaElsevier B.V., 139, pp. 127–136. doi: 10.1016/j.catena.2015.12.016.

Loescher HW, Oberbauer SF, Gholz HL and Clark DB 2003: Environmental controls on net ecosystem-level carbon exchange and productivity in a Central American tropical wet forest. Global Change Biology, 9(3), pp. 396–412. doi: 10.1046/j.1365-2486.2003.00599.x.

Luskin MS and Potts MD 2011: Microclimate and habitat heterogeneity through the oil palm lifecycle. Basic and Applied Ecology. doi: 10.1016/j.baae.2011.06.004.

Luyssaert S, Inglima I, Jung M, *et al.* 2007: CO2 balance of boreal, temperate, and tropical forests derived from a global database. Global Change Biology, 13(12), pp. 2509–2537. doi: 10.1111/j.1365-2486.2007.01439.x.

Malaysian Meteorological Department 2013: *Malaysian Meteorological Department*. MET Malaysia.Available at: http://www.met.gov.my/index.php?option=com_content&task=view&id=69&Itemid=160&limit=1&limitstart=1 (Accessed: 3 June 2015).

Malhi Y 2012: The productivity, metabolism and carbon cycle of tropical forest vegetation. Journal of Ecology, 100(1), pp. 65–75. doi: 10.1111/j.1365-2745.2011.01916.x.

Malhi Y, Pegoraro E, Nobre AD, Pereira MGP, Grace J, Culf AD and Clement R 2002: Energy and water dynamics of a central Amazonian rain forest. Journal of Geophysical Research Atmospheres, 107(20), p. 8061. doi: 10.1029/2001JD000623.

Massman WJ 2000: A simple method for estimating frequency response corrections for eddy covariance systems. Agricultural and Forest Meteorology, 104(3), pp. 185–198. doi: 10.1016/S0168-1923(00)00164-7.

Melling L 2013: Greenhouse gas (GHG) emission from tropical peatland. Planter, 89(1051), pp. 725–730.Available at: https://scholar.google.com/citations?view_op=view_citation&hl=en&user=dvbFMzYAAAAJ&cstart=20&pagesize=80&sortby=pubdate&citation_for_view=dvbFMzYAAAAJ:4TOpqqG69KYC.

Melling L, Goh KJ, Hatano R, Uyo LJ, Sayok A and Nik AR 2008: Characteristics of natural tropical peatland and their influence on C flux in Loagan Bunut National Park, Sarawak, Malaysia.in Proceedings of the 13th International Peat Congress: After Wise Use- The Future of PeatlandsTullamore, Ireland, pp. 226–229.

Melling L, Goh KJ, Uyo LJ, Sayok A and Hatano R 2007: Biophysical characteristics of tropical peatland. Proceedings of the Soil Science Conference of MalaysiaMukah,Sarawak: Malaysia Society of Soil Science, Selangor, 1917, pp. 17–19.

Melling L, Hatano R and Goh KJ 2005a: Methane fluxes from three ecosystems in tropical peatland of Sarawak, Malaysia. Soil Biology & Biochemistry, 37, pp. 1445–1453.

Melling L, Hatano R and Goh KJ 2005b: Soil CO2 flux from three ecosystems in tropical peatland of Sarawak, Malaysia. Tellus, Series B: Chemical and Physical Meteorology, 57(1), pp. 1–11. doi: 10.1111/j.1600-0889.2005.00129.x.

Miettinen J, Shi C and Liew SC 2017: Fire Distribution in Peninsular Malaysia, Sumatra and Borneo in 2015 with Special Emphasis on Peatland Fires. Environmental ManagementSpringer US, pp. 1–11. doi: 10.1007/s00267-017-0911-7.

Monda Y, Kiyono Y, Melling L, Damian C and Chaddy A 2015: Allometric equations considering the influence of hollow trees : A case study for tropical peat swamp forest in Sarawak. Tropics, 24(1), pp. 11–22. doi: 10.3759/tropics.24.11.

Moore S, Evans CD, Page SE, Garnett MH, Jones TG, Freeman C, Hooijer A, Wiltshire AJ, Limin SH and Gauci V 2013: Deep instability of deforested tropical peatlands revealed by fluvial organic carbon fluxes. NatureNature Publishing Group, 493(7434), pp. 660–3. doi: 10.1038/nature11818.

Murdiyarso D, Hergoualc'h K and Verchot L V 2010: Opportunities for reducing greenhouse gas emissions in tropical peatlands.in Proceedings of the National Academy of Sciences of the United States of America, pp. 19655–60. doi: 10.1073/pnas.0911966107.

Page SE and Hooijer A 2016: In the line of fire: the peatlands of Southeast Asia. Philosophical Transactions of the Royal Society B: Biological Sciences, 371(1696), p. 20150176. doi: 10.1098/rstb.2015.0176.

Page SE, Rieley JO and Banks CJ 2011: Global and regional importance of the tropical peatland carbon pool. Global Change Biology, 17(2), pp. 798–818. doi: 10.1111/j.1365-2486.2010.02279.x.

Page SE, Rieley JO, Shotyk W and Weiss D 1999: Interdependence of peat and vegetation in a tropical peat swamp forest. Philosophical transactions of the Royal Society of London. Series B, Biological sciences, 354(1391), pp. 1885–1897. doi: 10.1098/rstb.1999.0529.

Papale D, Reichstein M, Aubinet M, *et al.* 2006: Towards a standardized processing of Net

Ecosystem Exchange measured with eddy covariance technique: algorithms and uncertainty estimation. Biogeosciences, 3(4), pp. 571–583. doi: 10.5194/bg-3-571-2006.

Power S, Delage F, Chung C, Kociuba G and Keay K 2013: Robust twenty-first-century projections of El Niño and related precipitation variability. Nature, 502(7472), pp. 541–545. doi: 10.1038/nature12580.

Reichstein M, Falge E, Baldocchi D, *et al.* 2005: On the separation of net ecosystem exchange into assimilation and ecosystem respiration: Review and improved algorithm. Global Change Biology, 11(9), pp. 1424–1439. doi: 10.1111/j.1365-2486.2005.001002.x.

Rydin H and Jeglum JK 2015: *The Biology of Peatlands*. The Biology of Peatlands. doi: 10.1093/acprof:osobl/9780199602995.001.0001.

Schimel DS, House JI, Hibbard K a, *et al.* 2001: Recent patterns and mechanisms of carbon exchange by terrestrial ecosystems. Nature, 414(6860), pp. 169–172. doi: 10.1038/35102500.

Song-Miao F, Wofsy SC, Bakwin PS, Jacob DJ and Fitzjarrald DR 1990: Atmosphere-biosphere exchange of CO2 and O3 in the central Amazon forest. Journal of Geophysical Research, 95(D10), p. 16,816-851,864. doi: 10.1029/JD095iD10p16851.

Stockwell CE, Jayarathne T, Cochrane MA, *et al.* 2016: Field measurements of trace gases and aerosols emitted by peat fires in Central Kalimantan, Indonesia, during the 2015 El Ni??o. Atmospheric Chemistry and Physics, 16(18), pp. 11711–11732. doi: 10.5194/acp-16-11711-2016.

Stuart Chapin F, Matson PA and Vitousek PM 2012: *Principles of terrestrial ecosystem ecology*. Principles of Terrestrial Ecosystem Ecology. doi: 10.1007/978-1-4419-9504-9.

Sugawara M 1979: Automatic calibration of the tank model / L'étalonnage automatique d'un modèle à cisterne. Hydrological Sciences Bulletin, 24(3), pp. 375–388. doi: 10.1080/02626667909491876.

Sundari S, Hirano T, Yamada H, Kusin K and Limin S 2012: Effect of groundwater level on soil respiration in tropical peat swamp forests. Journal of Agricultural Meteorology, 68(2), pp. 121–134. doi: 10.2480/agrmet.68.2.6.

Tan KP, Devi K, Bin I and Philip A 2011: EVALUATION OF MODIS GROSS PRIMARY PRODUCTIVITY OF TROPICAL OIL PALM IN SOUTHERN PENINSULAR MALAYSIA Department of Remote Sensing , Faculty of Geoinformation and Real Estate , Universiti Teknologi. 2011 Ieee International Geoscience and Remote Sensing Symposium, pp. 756–759.

Ueyama M, Hirata R, Mano M, Hamotani K, Harazono Y, Hirano T, Miyata A, Takagi K and Takahashi Y 2012: Influences of various calculation options on heat, water and carbon fluxes determined by open- and closed-path eddy covariance methods. Tellus B, 64(0). doi: 10.3402/tellusb.v64i0.19048.

UNDP 2006: *Malaysia's Peat Swamp Forets: Conservation and Sustainable Use*. United Nations Development Programme (UNDP), Malaysia. doi: 10.1017/CBO9781107415324.004.

Vickers D and Mahrt L 1997: Quality control and flux sampling problems for tower and

aircraft data. Journal of Atmospheric and Oceanic Technology, 14(3), pp. 512–526. doi: 10.1175/1520-0426(1997)014<0512:QCAFSP>2.0.CO;2.

Webb EK, Pearman GI and Leuning R 1980: Correction of flux measurements for density effects due to heat andwater vapour transfer. Quarterly Journal of the Royal Meteorological Society, 106, pp. 85–100.

Wieder WR, Cleveland CC and Townsend AR 2009: Controls over leaf litter decomposition in wet tropical forests. Ecology. doi: 10.1890/08-2294.1.

Wilczak J, Oncley S and Stage S 2001: Sonic Anemometer Tilt Correction Algorithms. Boundary-Layer Meteorology, 99(1), pp. 127–150.

Wong GX, Hirata R, Hirano T, Kiew F, Aeries EB, Musin KK, Waili JW, Lo KS and Melling L 2018: Micrometeorological measurement of methane flux above a tropical peat swamp forest. Agricultural and Forest Meteorology. doi: 10.1016/j.agrformet.2018.03.025.